AWARD NUMBER: W81XWH-19-1-0599

TITLE: Overcoming Immunotherapy Resistance in Breast Cancer Using RT-Mediated Immunomodulation

PRINCIPAL INVESTIGATOR: Stephen Shiao

CONTRACTING ORGANIZATION: Cedars-Sinai Medical Center, Los Angeles, CA

REPORT DATE: October 2021

TYPE OF REPORT: Annual

PREPARED FOR: U.S. Army Medical Research and Development Command
Fort Detrick, Maryland 21702-5012

REPORT DOCUMENTATION PAGE

Form Approved
OMB No. 0704-0188

1. REPORT DATE	2. REPORT TYPE	3. DATES COVERED
October 2021	Annual	15Sep2020-14Sep2021

4. TITLE AND SUBTITLE

Overcoming Immunotherapy Resistance in Breast Cancer Using RT-Mediated Immunomodulation

5a. CONTRACT NUMBER
W81XWH-19-1-0599

5b. GRANT NUMBER

5c. PROGRAM ELEMENT NUMBER

6. AUTHOR(S)

Stephen Shiao

E-Mail:

5d. PROJECT NUMBER

5e. TASK NUMBER

5f. WORK UNIT NUMBER

7. PERFORMING ORGANIZATION NAME(S) AND ADDRESS(ES)

Cedars-Sinai Medical Center,
8700 Beverly Blvd, Los Angeles, CA, 90048

8. PERFORMING ORGANIZATION REPORT NUMBER

9. SPONSORING / MONITORING AGENCY NAME(S) AND ADDRESS(ES)

U.S. Army Medical Research and Development Command
Fort Detrick, Maryland 21702-5012

10. SPONSOR/MONITOR'S ACRONYM(S)

11. SPONSOR/MONITOR'S REPORT NUMBER(S)

12. DISTRIBUTION / AVAILABILITY STATEMENT
Approved for Public Release; Distribution Unlimited

13. SUPPLEMENTARY NOTES

14. ABSTRACT
Breast cancer generally exhibits low response rates to immunotherapy such as PD-1/PD-L1 blockade for multiple reasons including tumor-mediated immune suppression and poor immunogenicity. We sought to change the responsiveness of breast tumors to anti-PD-1 therapy by reshaping the tumor immune microenvironment using focal radiation (RT). Irradiation of breast tumors elicits direct killing of malignant cells, but more importantly generates an anti-tumor immune response. This immune reaction is a critical mediator of both primary tumor control and abscopal responses, though the cellular and molecular dynamics within the immune compartment following treatment are incompletely understood. We elucidated these changes using single-cell sequencing in a preclinical model of breast cancer. We found that immediately following RT intratumoral immune cells are largely eliminated and a de novo inflammatory response initiated. The ensuing response consists of activated cytotoxic CD8+ T cells and CD11b+ myeloid/macrophages, but also induced regulatory T cells and inhibitory signals including PD-1 on T cells and PD-L1 on macrophages. We found that RT synergizes with PD-1 blockade through its ability to alleviate intratumoral immunosuppression and stimulate the production of cytotoxic T cells through the generation of a hyperphagocytic, cytotoxic and antigen presenting macrophage phenotype. Examination of biopsies from breast cancer patients undergoing neoadjuvant anti-PD-1 and RT revealed similar changes. We observed enhanced macrophage mediated killing and antigen presentation leading to increased numbers and activation of intratumoral immune responses across more than 80% of patients examined. These observations support the notion that RT mediated changes in the tumor immune microenvironment enhance the sensitivity of breast tumors to checkpoint blockade.

15. SUBJECT TERMS
Breast Cancer, Radiation Therapy, Immune Checkpoint Blockade, Single Cell Sequencing

16. SECURITY CLASSIFICATION OF:			17. LIMITATION OF ABSTRACT	18. NUMBER OF PAGES	19a. NAME OF RESPONSIBLE PERSON
a. REPORT	b. ABSTRACT	c. THIS PAGE			USAMRMC
Unclassified	Unclassified	Unclassified	Unclassified	37	19b. TELEPHONE NUMBER *(include area code)*

TABLE OF CONTENTS

1. INTRODUCTION:

Most breast cancers remain resistant to immunotherapy in part through the establishment of an immunosuppressive microenvironment by malignant cells. Radiation therapy (RT) can dramatically alter the immune microenvironment of tumors both through elimination of the existing immune cells within tumors and stimulation of a de novo immune response. Thus, *our overall hypothesis is that combining focal breast RT with immunotherapy will increase the efficacy of immunotherapy for breast cancer by favorably reprogramming the tumor immune microenvironment of breast tumors*. Given the resistance of most breast cancers to immunotherapy and the ability of RT to alter the tumor immune microenvironment, we proposed three aims to understand and target the mechanisms by which RT shapes the immune microenvironment of breast tumors to augment antitumor immune responses. In the first two aims we proposed to characterize the local and systemic immune responses to RT and anti-PD1 a murine model of breast cancer, and then to use the same model and knockout mouse lines lacking different immune cells to elucidate the mechanisms by which RT improves immunotherapy responses. In a final aim we proposed to examine the role of RT in altering the response to anti-PD1 therapy in a human breast cancer trial of neoadjuvant RT and immunotherapy

2. KEYWORDS:

Breast cancer, Single cell sequencing (SCseq), Immunotherapy, Radiation Therapy (RT), Macrophage, CD8+ T cell, CD4+ T cell, B cell

3. ACCOMPLISHMENTS:

What were the major goals of the project?

The three main goals for this project are (1) Characterize the impact of RT-induced changes in the tumor immune microenvironment on the efficacy of immunotherapy both locally and systemically, (2) Define mechanism(s) of RT-mediated modulation of tumor responses to immunotherapy and (3) Examine the role of RT in modulating the efficacy of immunotherapy in a human breast cancer trial of neoadjuvant RT and immunotherapy.

What was accomplished under these goals?

In the previous reporting period, we obtained IACUC/ACURO approval for our mouse studies as well as IRB/HRPO approval for our human trial (Milestones 1A and 1B). We began our animal studies as scheduled and began enrolling patients in our trial completing the Phase Ib (first 10 patients) in the Year 1 (Milestone 2C).

In Year 2, we continued to experience some COVID-related delays for the first half of Year 2 (September 2020 – March 2021) which slowed the mouse experiments and accrual to our trial, however with the reopening of the laboratories and resumption of full trial activity at our institution in April we have make good progress on completing the goals set forth in our project.

Since last year, we have completed both the single tumor, single dose radiation with anti-PD-1 and the single tumor, multi-dose radiation study with anti-PD-1 (SA1, MT1, Subtasks 4 and 5). The two tumor, single dose and multi dose RT with anti-PD-1 studies are currently underway (SA1, MT2, Subtasks 1 and 2) and the single tumor, single dose radiation study with anti-PD-1 and anti-CSF1R (SA2, MT1, Subtask 1) which we anticipate completing in the first half of the coming year.

We have also continued to enroll patients and over Year 2 we enrolled 28 patients, however due to COVID-related issues 8 patients were withdrawn from the trial. We requested and received a funded extension of the trial to replace those 8 patients and have continued to enroll (SA3, MT3, Subtask 2). We anticipate completing enrollment and follow up in middle of Year 4 (month 42) as planned with the current extension.

Though trial enrollment and laboratory work was suspended for part of the period covered by this report, we were able to complete analysis of the biopsy specimens that were collected on the Phase Ib portion of the trial and the first mouse studies with the single-tumor, single-dose with PD-1 samples (Milestone 2D).

Each of the detailed goals to be completed up to and including this reporting period are noted in the table below. Following the table is a detailed descriptions of the scientific findings from these studies.

Specific Aim 1: Characterize the impact of RT-induced changes in the tumor immune microenvironment on the efficacy of immunotherapy both locally and systemically	**Timeline**	**Site 1** (Stephen Shiao, MD, PhD)	**Site 2** (Simon Knott, PhD)
Major Task 1: Effects of different doses of RT on the efficacy of PD-1/PD-L1-directed immunotherapy	Months		
Subtask 1: Local IACUC Approval	0	Dr. Shiao	
Subtask 2: Train new staff.	1-3	Dr. Shiao	
Subtask 3: Complete evaluation sequencing (scSeq) pipelines & train new staff.	1-3		Dr. Knott
Subtask 4: Single tumor, single dose radiation study with anti-PD-1. • Perform radiation exposure and immunotherapy administration, collect blood samples/fecal pellets and tumor tissue for scSeq, histology, flow cytometry of immune and non-immune tumor components. • scSeq library preparation, quality control (QC), pooling and sequencing • scSeq data analysis	4-7 7 8-9	Dr. Shiao	 Dr. Knott Dr. Knott
Subtask 5: Single tumor, multi-dose radiation study with anti-PD-1 • Perform multi-dose radiation exposure and immunotherapy administration, collect blood samples/fecal pellets and tumor tissue for scSeq, histology, flow cytometry of immune and non-immune tumor components. • scSeq library preparation, QC, pooling and sequencing • scSeq data analysis	8-11 11 12-13	Dr. Shiao	 Dr. Knott Dr. Knott
Milestone #1A: ACURO Approval.	4	Dr. Shiao	
Major Task 2: Effect of RT on immunotherapy-induced systemic anti-tumor immunity			

Subtask 1: Two tumor, single dose radiation study with anti-PD-1 • Perform radiation exposure and immunotherapy administration, collect blood samples/fecal pellets and tumor tissue for scSeq, histology, flow cytometry of immune and non-immune tumor components. • scSeq library preparation, quality control (QC), pooling and sequencing • scSeq data analysis	11-14 14 15-16	Dr. Shiao	 Dr. Knott Dr. Knott
Subtask 2: Two tumor, multi-dose radiation study with anti-PD-1 • Perform multi-dose radiation exposure and immunotherapy administration, collect blood samples/fecal pellets and tumor tissue for scSeq, histology, flow cytometry of immune and non-immune tumor components. • scSeq library preparation, QC, pooling and sequencing • scSeq data analysis	14-17 17 18-19	Dr. Shiao	 Dr. Knott Dr. Knott
Milestone #2A: Complete processing & analysis of first 640 animals (effects of different types of radiation on anti-PD-1 immunotherapy). Expect to find significant changes in both immune and non-immune populations. *Milestone #2B: Co-author manuscript on the effects of radiation on the tumor microenvironment.*	17 19-25	Dr. Shiao	Dr. Knott
Specific Aim 2: Define mechanism(s) of RT-mediated modulation of tumor responses to immunotherapy			
Major Task 1: Investigation of the role of innate immune responses			
Subtask 1: Single tumor, single dose radiation study with anti-PD-1 and anti-CSF1R (to deplete macrophages) • Perform radiation exposure and immunotherapy administration, collect blood samples/fecal pellets and tumor tissue for scSeq, histology, flow cytometry of immune and non-immune tumor components. • scSeq library preparation, quality control (QC), pooling and sequencing • scSeq data analysis	17-20 20 21-22	Dr. Shiao	 Dr. Knott Dr. Knott
Subtask 2: Single tumor, single dose radiation study in CD11c-DTR mice with anti-PD-1 and diptheria toxin (to deplete dendritic cells). • Perform radiation exposure and immunotherapy administration, collect blood samples/fecal pellets and tumor tissue for scSeq, histology, flow cytometry of immune and non-immune tumor components. • scSeq library preparation, quality control (QC), pooling and sequencing • scSeq data analysis	20-23 23 24-25	Dr. Shiao	 Dr. Knott Dr. Knott

Milestone #3A: Complete analysis of changes in the tumor microenvironment with RT and anti-PD-1 therapy in the absence of macrophages or dendritic cells. Expect to find significant changes in both immune and non-immune parameters.	23	Dr. Shiao	Dr. Knott
Specific Aim 3: Examine the role of RT in modulating the efficacy of immunotherapy in a human breast cancer trial of neoadjuvant RT and immunotherapy			
Major Task 1: Conduct initial phase Ib trial to assess the safety of neoadjuvant RT and immunotherapy			
Subtask 1: Submit documents for local IRB review and approval	1-4	Dr. Shiao	
Subtask 2: Submit IRB approval and necessary documents for HRPO Review	4-7	Dr. Shiao	
Milestone #1B: HRPO Review and Approval	4-7	Dr. Shiao	
Subtask 3: Enroll first 10 patients on the phase Ib (Key Collaborators: Dr. McArthur, Basho, Giuliano and Karlan)	7-13	Dr. Shiao	
Subtask 4: scSeq analysis of clinical trial biopsies • scSeq library preparation, QC, pooling and sequencing • scSeq data analysis	 7-13 14-15		 Dr. Knott Dr. Knott
Subtask 5: Complete preliminary evaluation of safety determination and make necessary modifications to being Phase II portion of trial (Biostatistician: Andre Rogatko, Key Collaborators: Dr. McArthur, Basho, Giuliano and Karlan)	13-15	Dr. Shiao	
Subtask 6: Consolidate analysis of scSeq, flow cytometry, immunohistochemistry and microbiome data from patient samples for Phase Ib trial	15-19	Dr. Shiao	Dr. Knott
Milestone #2C: Completion of Phase Ib trial and statistical analysis *Milestone #2D: Complete analysis of patient samples from Phase Ib trial. Anticipate seeing changes in immune microenvironment following RT and limited addressable safety issues from two agents with known toxicity profiles.*	13-15 15-19	Dr. Shiao	Dr. Knott
Major Task 3: Conduct phase II trial to assess the efficacy of neoadjuvant RT and immunotherapy			
Subtask 1: Submit any necessary protocol modifications to local IRB and HRPO to address safety issues seen in Phase Ib trial	15-18	Dr. Shiao	
Subtask 2: Enroll 40 patients on the phase II trial (Key Collaborators: Dr. McArthur, Basho, Giuliano and Karlan)	18-36	Dr. Shiao	

Murine Studies

Analyses of previously acquired data

To elucidate how RT changes the intratumoral leukocyte population following radiation therapy (RT), we previously applied single cell RNA sequencing (scSeq) to the immune cells of orthotopic E0771 murine mammary tumors following a single fraction of focal irradiation (16 Gray, Gy). The beam arrangement and dose selected ensured the treatment encompassed the entire tumor while avoiding surrounding tissue, and that RT delayed tumor growth and prolonged survival (Fig 1a). CD45^{+} cell populations from tumors that were irradiated 3, 7, 10- and 14-days prior at sizes of ~1 cm^3 were collected and analyzed.

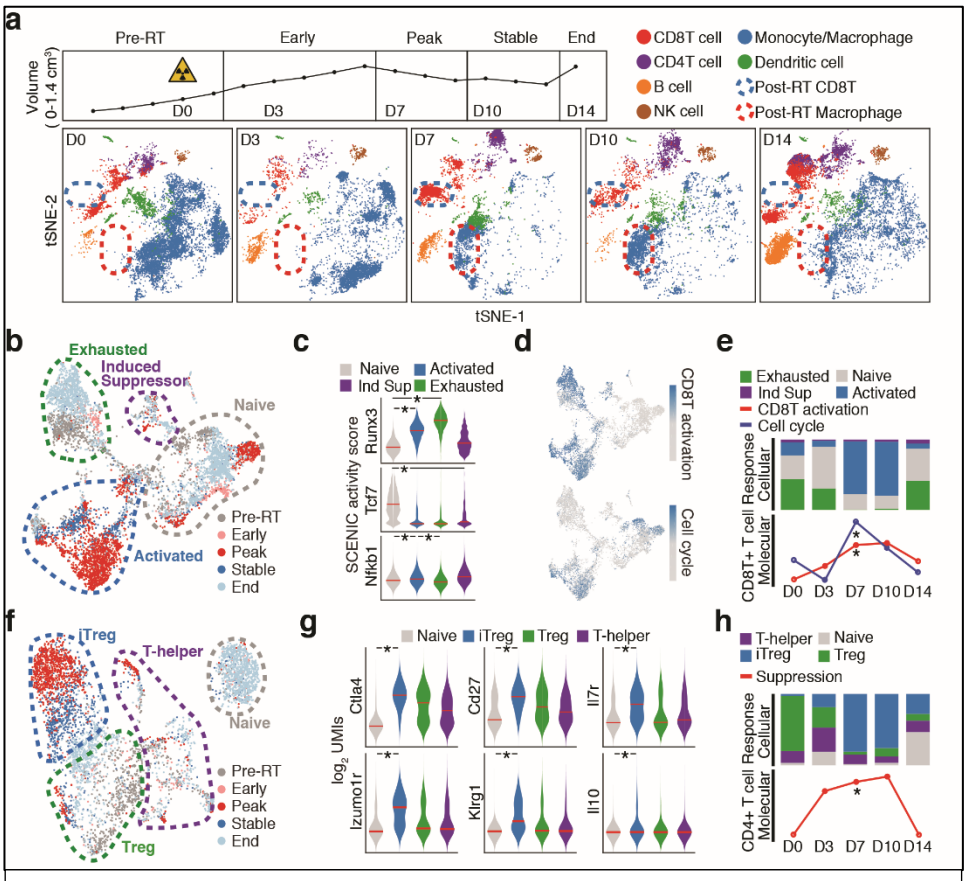

Figure 1. Radiation therapy perturbs tumor immune microenvironment through the activation of CD8 T-cells with a compensatory CD4 regulatory T-cell response. **(a),** Representative radiation-treated orthotopic E0771 tumor growth curve (top) and corresponding tSNE embedding of the tumor immune microenvironment at indicated time points (bottom). Cells are colored by cell type and dashed lines highlight RT induced changes in the innate and adaptive arms. **(b),** UMAP embedding of CD8 T-cells (CD8T) from **a**. **(c),** Transcription factors differentially activated in the CD8T population, as predicted by SCENIC (Wilcoxon rank sum test, * $p < 10^{-15}$). **(d),** Diffusion component (DC) scores corresponding to CD8T activation and cell cycle overlaid on UMAP embedding from **d**. **(e),** Composition of CD8T subpopulations, as annotated in **d**, (top) and average DC score of CD8Ts, as shown in **d**, (bottom) across timepoints (Wilcoxon rank sum test, * $p < 10^{-100}$ D7 vs D0). **(f),** UMAP embedding of intra-tumoral CD4 T-cells (CD4T). **(g),** Key genes differentially expressed in induced regulatory T-cells (iTreg) (Wilcoxon rank sum test, * FDR < 10^{-15}). **(h),** Composition of CD4T subpopulations, as annotated in **g**, (top) and average DC score of CD4Ts (bottom) across timepoints (Wilcoxon rank sum test, * $p < 10^{-95}$ D7 vs D0).

As previously described[4], we found that the majority of immune cells at baseline were T cells and macrophages, though others including NK cells, B cells and Dendritic Cells (DC) were also present (Fig 1a). Following irradiation, we observed a dramatic reshaping within both the T cell and macrophage compartments, with the elimination of most baseline populations completely at Day 3 followed by the appearance of new populations starting at Day 3 and continuing through Day 10 (Fig. 1a). Interestingly, the original immune cell repertoire was largely restored by Day 14.

To examine the functional state of the CD8+ T cells (CD8T) following RT, we used established markers to classify constituents as naïve, activated, exhausted or induced suppressive and then tracked their proportions within the tumor over time (Fig. 1b). Naïve cells were low for CD44 and CD69 and high for CD62L, and an analysis of transcription factor activity scores suggested this program was driven by Tcf7 (Fig. 1c). Activated and exhausted cells both expressed a Runx3 driven activation program corresponding to diffusion component 1, that harbored the genes Granzyme B, perforin, CD69 (Fig. 1c-d). Differentiating these groups were Lag3- and Tim3-expression in the exhausted cells and a proliferative signature in the activated group, corresponding to diffusion component 3 (Fig. 1d). Overall, the naïve T cell population expanded 1.5x by day 3 after RT, while the activated population dominated Days 7 and 10. The activation signature wanes by day 14 with the cellular and molecular signatures returning to baseline. This timeline mirrors other cytotoxic T cell responses such as viral infections[6] indicating that RT triggers a response akin to a de novo immune response in tumors.

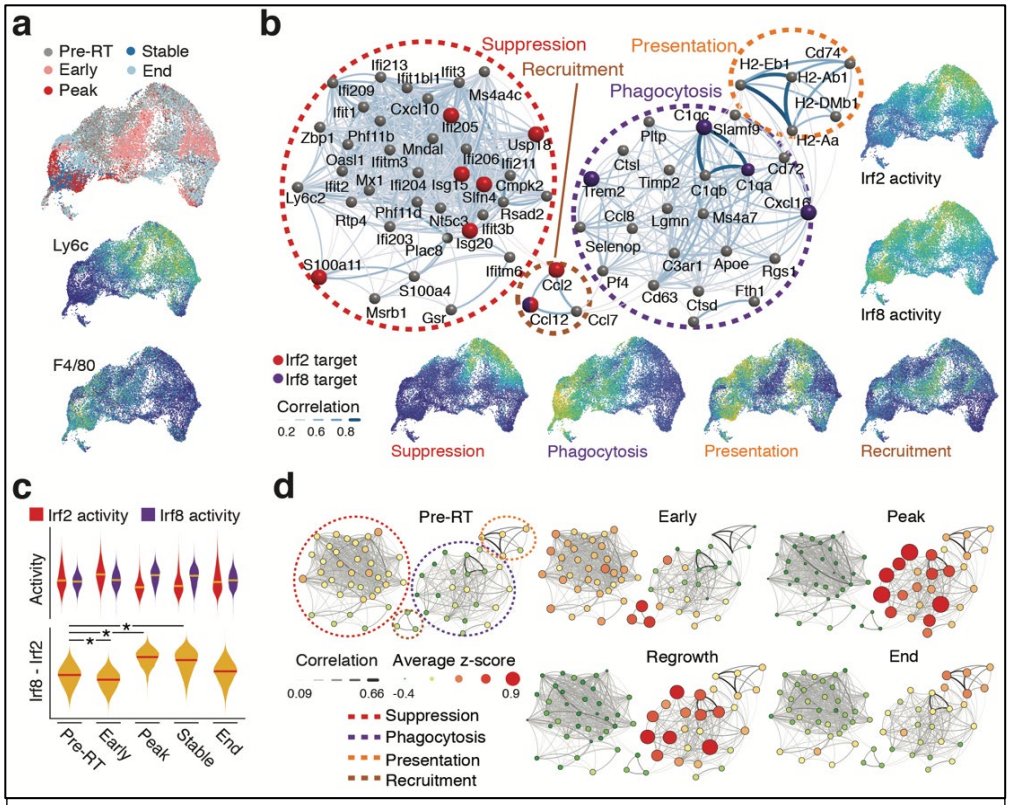

Figure 2. Radiation therapy induces an acute transition of intra-tumoral macrophages from a suppressive to a phagocytic phenotype. (a), UMAP embedding of intra-tumoral macrophages colored by time point (top) and expression of key phenotypic markers overlaid (bottom). **(b),** Gene network correlation graph derived de-novo from macrophage data with core modules highlighted, weight of edges determined by inter-gene correlation, and nodes colored if predicted to be downstream targets of Irf2 or Irf8, as determined by SCENIC regulons. The network graph is surrounded by overlays of median core module expression and Irf2 and Irf8 SCENIC activity scores on the UMAP from **a**. **(c),** Irf2 and Irf8 activation, as predicted by SCENIC, and difference in activation status in macrophages across timepoints (Wilcoxon rank sum test, * $p < 2.9x10^{-146}$). **(d),** The same network graph as in **b**, but with node size and color determined by the average z-scored expression of the node at each time point.

A similar analysis of CD4+ T cells (CD4T) identified naïve, T-helper, regulatory T cells (Tregs), but the most interesting change in the CD4T compartment was the appearance of an "induced" Treg (iTreg) population that strongly peaks through Days 7 and 10 (Fig. 1f-h). iTregs express a unique suppressive signature harboring regulatory genes such as IL-10, Izumo1r, CD27 and Klrg1, which is defined by the first diffusion component of the $CD4^+$ population and is similar to that of TGFβ1-induced regulatory T cells described previously[7]. Our findings support the notion that the strong inflammatory response induced by RT drives a compensatory regulatory response, which other groups have shown is a critical mediator of local and systemic anti-tumor immunity following RT[8].

We next examined monocyte/macrophage cells using a gene co-expression analysis and identified 4 major expression modules. These consisted of Ly6c^{-} ^{hi}F4/80^{lo} suppressive and Ly6c^{lo}F4/80^{hi} phagocytic modules with intermediate Ccl2^{hi} recruitment and MHC-Class II^{hi} presentation modules (Fig. 2a & b). Additionally, we identified Irf2 and Irf8 as potential regulators of the suppressive and phagocytic modules, respectively (Fig. 2b). Irf2 expression in macrophages drives an anti-inflammatory program[9] whereas Irf8 drives anti-tumor immunity[10]. In comparison to baseline, macrophages were most significantly altered in their expression program after 7 and 10 days. Following RT, an Irf2^{lo}Irf8^{hi} phagocytic population overtook the compartment and remained beyond Day 10 (Fig. 2c & d). However, Irf2 and Irf8 levels rebalanced by Day 14, returning module expression to baseline levels. Our findings indicate RT initiates a transient reprogramming of macrophages from an immunosuppressive, homeostatic phenotype to a cytotoxic, antigen-presenting phenotype. The reversion to baseline is likely driven by the suppressive signals produced within macrophages consuming apoptotic cells[11].

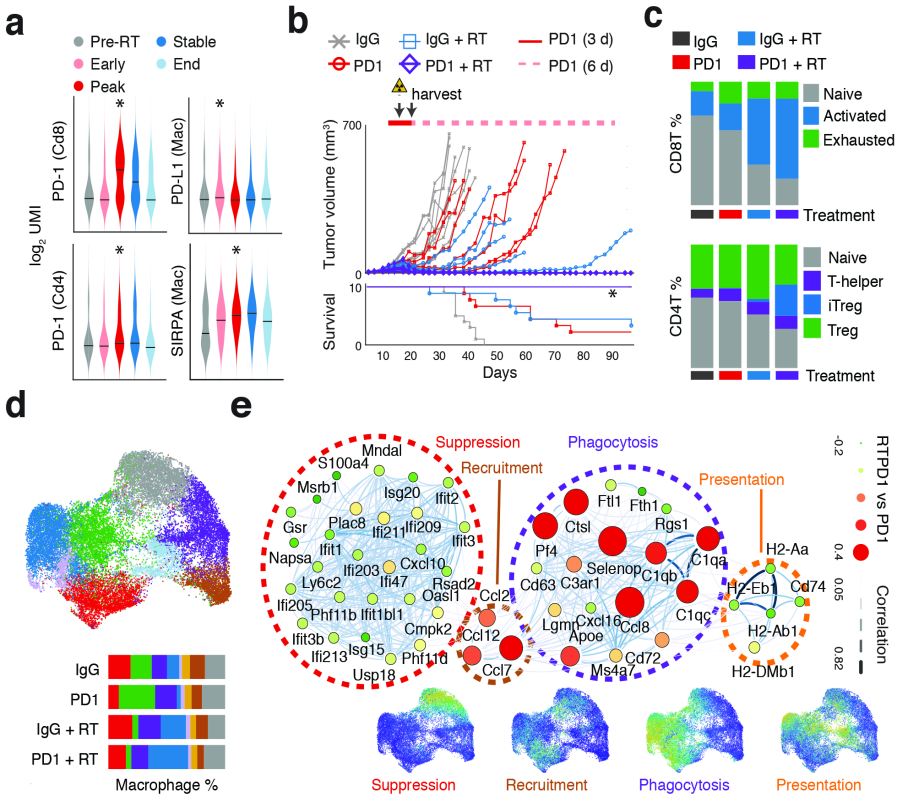

Figure 3. Combination anti-PD-1 and radiation treatment induces durable anti-tumor response characterized by a robust CD8 T-cell activation and macrophage phagocytic/presentation phenotype. (a), Expression of key immune checkpoint molecules in intra-tumoral CD8 and CD4 T-cells (CD8T and CD4T) and macrophages (Mac) following radiation therapy. (Wilcoxon rank sum test, PD-1 CD8T D7 vs D0 FDR = 1.2E^{-50}, PD-1 CD4T D7 vs D0 FDR = 1.1x10^{-16}, PD-L1 Macs D3 vs D0 FDR = 3.9x10^{-193}, SIRPA Macs D7 vs D0 FDR = 5.5x10^{-132}). **(b),** Individual tumor growth curves (top) and survival curve (bottom) for orthotopic E0771 tumor bearing mice administered control antibody (IgG), anti-PD-1 (PD1), IgG and radiation (IgG+RT), or PD1 and RT (PD1+RT) (log-rank test, * p = 2.2x10^{-8}). **(c)**, Composition of intra-tumoral CD8T (top) and CD4T (bottom) subpopulations in indicated treatment groups. **(d),** UMAP embedding of macrophages from all samples combined and colored by cluster (top) accompanied by the composition of macrophage clusters in indicated treatment groups colored as in UMAP (bottom). **(e),** Macrophage gene network correlation graph with core modules highlighted, weight of edges determined by inter-gene correlation, and nodes sized/colored by the average z-scored (across macrophages in PD1+RT and PD1 groups) expression of the node (top). Expression of each core module overlaid on the UMAP from **d** (bottom). Data in **c, d,** and **e** are from tumors harvested where indicated in **b**, i.e. 5 days after radiation treatment, where two independent cohorts of mice were analyzed, combining two tumors from each treatment group for each cohort.

To better understand the activation pathways governing this RT-mediated transformation we performed a focused examination of known checkpoint proteins and found that RT upregulated PD-1 in CD8Ts, PD-L1 in CD4Ts and PD-L1 and SIRPA in macrophages (Fig. 3a). This data and previous studies in melanoma[12] and NSCLC[13] showing synergy between RT and immune checkpoint

blockade prompted us to ask if targeting the PD1/PD-L1 axis in the context of RT could promote further immune mediated killing in our murine model of breast cancer.

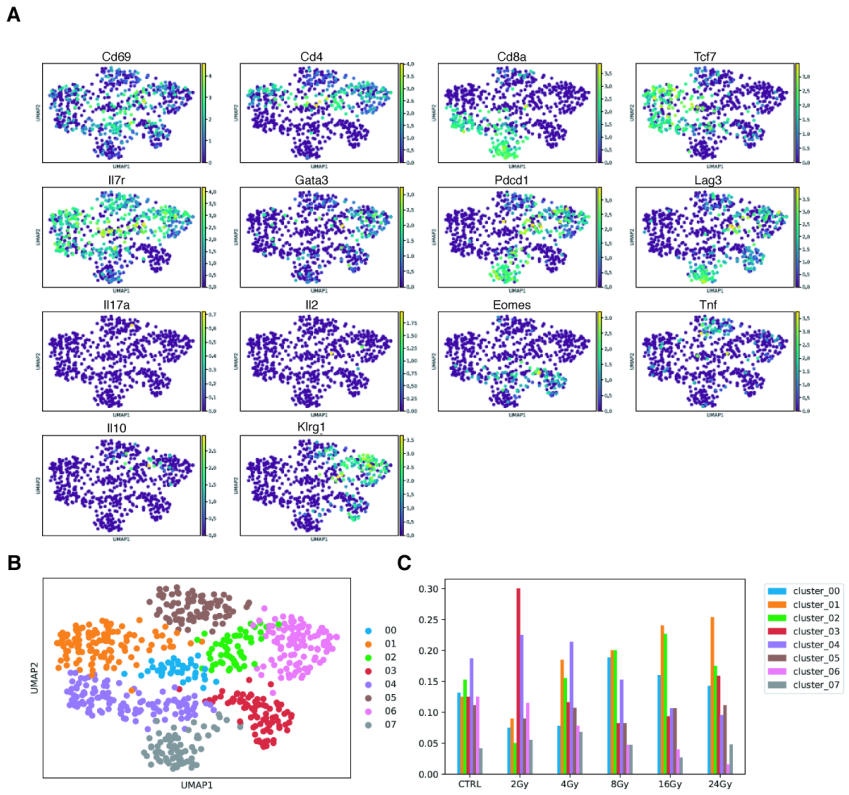

Figure 4. Single-cell analysis of the T cell compartment in murine EO771 mammary tumor T cell phenotypes following different levels of single dose focused radiation. A) Functional markers of T cells showing markers for Naïve (Cd69, Tcf7, Il7r) and activated or exhausted (Gata3, Pdcd1, Lag3) T cells. B) Unbiased T cell clusters. C) Proportions of T cells of each cluster/phenotype following each radiation dose, showing increased numbers of naïve Cd4 and Cd8 T cells (cluster 1 and cluster 4) at 4 Gy and increased numbers of activated Cd4 and Cd8 (cluster 2 and cluster 0, respectively) T cells at 8 and 16 Gy.

Acquisition and Analysis of Murine Data for Current Project

As part of Aim 1 of this current application, we enrolled orthotopic tumor bearing mice into each of four study arms, which included IgG control antibody, anti-PD1 antibody, IgG control antibody with RT and anti-PD1 antibody with RT. Control tumors grew quickly, with all mice requiring euthanasia by Day 45 (Fig 3b). Mice receiving RT or anti-PD1 alone saw tumor shrinkage followed by regrowth. In contrast, animals administered the combination showed complete tumor regression and 100% survival beyond 90 days.

To study the changes in the immune compartment underlying this synergism, we extracted tumors on Day 5 following RT and where three doses of PD1 blocking antibody had been administered and analyzed leukocytes with scSeq. As was observed previously, RT alone increased the proportion of activated $CD8^+$ T cells, which was not seen with PD1 blockade, despite the associated increased survival (Fig. 3e). Instead, PD1 blockade expanded the exhausted CD8T population at the expense of naïve T cells. Combination therapy boosted activated CD8Ts compared to RT alone with a corresponding decrease in naïve CD8Ts. Interestingly, RT uniquely induced an iTreg population and the combination treatment drove an expansion in this group that was five times greater than with RT alone. Our studies show that combining RT with anti-PD1 augments the numbers and function of cytotoxic T cells similar to other preclinical breast models that have demonstrated synergy with this combination[14]. However, we also show there is a simultaneous increase in a regulatory T cell population, which likely governs the ability of RT to induce an abscopal response beyond the irradiated tumor.

RT again also uniquely drove expansion of $F4/80^{hi}$ and $Ly6c^{lo}$ macrophages, and a gene co-expression analysis determined the phagocytic and presentation modules were activated in this population (Fig 3d, e). PD1 blockade produced a similar phenotype, but with tempered phagocytic and recruitment module activity and slightly higher presentation gene levels. When combined, RT

and PD1 blockade collaborated for a specific expansion (20%) of the RT-associated macrophage population with elevated phagocytic and antigen presenting capacity (Fig. 3d). This activity likely drives the enhanced cytotoxic response following RT as tumor-associated macrophages are important potential drivers of anti-tumor immunity[15].

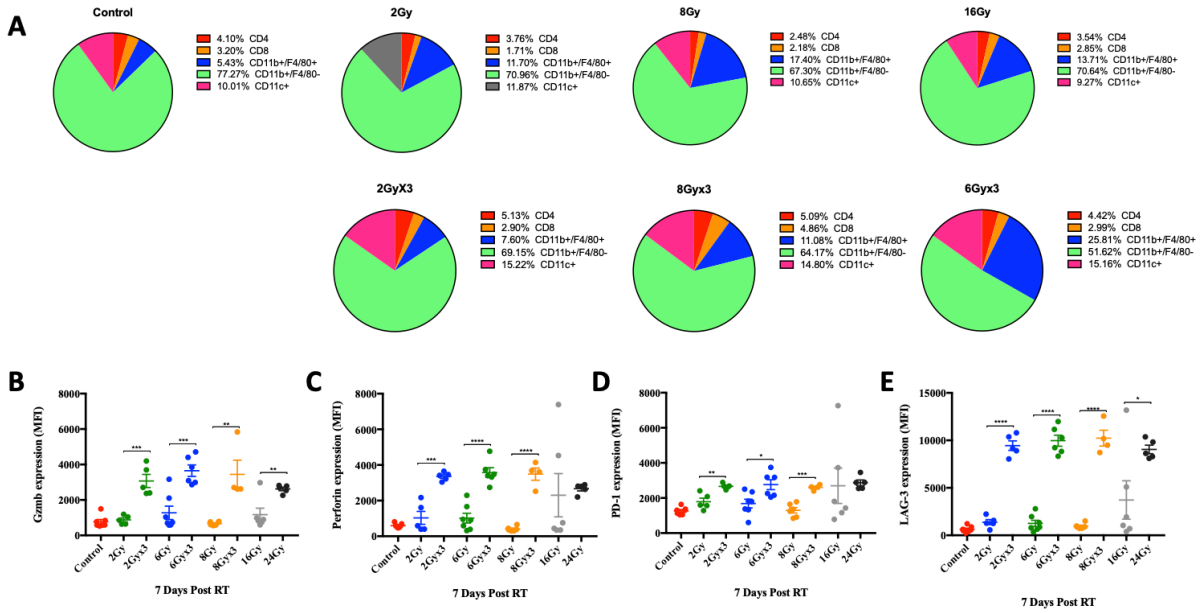

Figure 5. Murine EO771 mammary tumor immune profiles following different levels of single dose and multi-fraction focused radiation. A) The percentage of T cells and myeloid-macrophages in the CD45+ immune compartment were analyzed by flow cytometry. Mean fluorescence intensity (MFI) of activation markers Granzyme B (GrnB) (B), Perforin (C), suppressive marker PD-1 (D) and exhaustion marker LAG-3 (E) was determined on CD8+ T cells.

Single-cell analysis of various different RT doses showed that doses above 4 Gy were the most effective immunostimulatory single-dose producing slightly more CD8+ T cells with less exhausted (LAG-3+) phenotypes. Flow cytometry comparing single-fraction to multi-fraction doses revealed that multi-fraction doses generally are more immunostimulatory and among the multi-fraction doses 6-8 Gy x 3 were the most effective immunostimulatory multi-doses producing more activated CD8+ T cells though these also carried high expression of PD-1 and LAG-3 (Figure 5).

SCseq Analysis of Immune Cells from Phase IB and II Clinical Trial

As listed in the Aim 3 of our SOW, we designed and executed a phase 1b/II clinical trial to study the combination of the anti-PD1 antibody pembrolizumab in combination with RT in the neoadjuvant setting for women with triple-negative breast cancer (TNBC). Additionally, we have enrolled nearly 20 patients into our phase II trial Aim 3 Major Task 2, and have begun to analyze thses samples. Here we present analysis from the first 11 of the newly diagnosed TNBC patients received pre-operative pembrolizumab, followed three weeks later by pembrolizumab with RT (24 Gy/3 fractions) to the primary breast tumor only, which was then followed by standard-of-care chemotherapy, surgery and RT (Fig. 4a). Of the 11 patients evaluated, 8 (82%) showed a pathologic complete response at the time of surgery and three of the four baseline node-positive patients were cleared of metastases, demonstrating the potential of the combination.

We examined the immune and non-immune compartments prior to and following anti-PD1 and anti-PD1 with RT by performing scSeq on CD45^{+} and CD45- cells obtained from research biopsies taken from each patient at baseline, 3 weeks after pembrolizumab and 3 weeks after combined RT and pembrolizumab (Figure 7A, B). In total we analyzed nearly 900,000 total cells.

As in orthotopic EO771 tumors, macrophages, CD8+ and CD4+ T cells were found to be in high abundance in most human TNBC tumors, and the variation within these populations appeared driven by many of the same programs as were described in murine cells (Figure 6 and 7C). However, inter-tumor heterogeneity was also found to be a major source of variation (Data not shown).

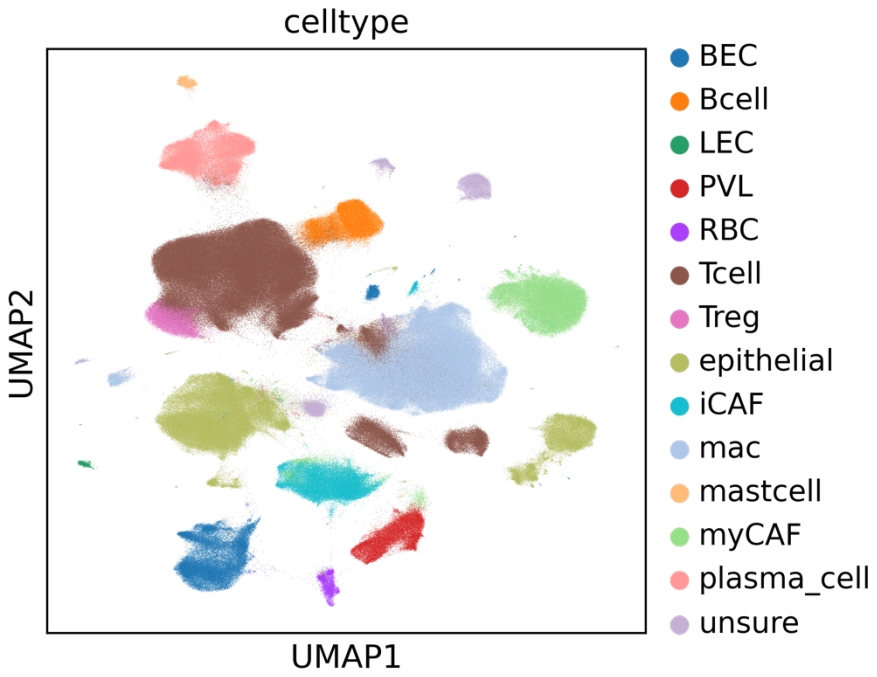

Figure 6. UMAP embedding and clustering of all ~900,000 cells isolated from clinical trial biopsies. Immune cells were identified and annotated as was described in past reports. Cells lacking CD45 expression have been annotated based on markers found to be differentially expressed within the corresponding cells. These populations include Blood Endothelial Cells (BEC), Lymphatic Endothelial Cells (LEC), Pericytes (PVL), Red Blood Cells (RBC), epithelial cells, Inflammatory Cancer Fibroblasts (iCAFs) and myofibroblasts (myCAFs). Analysis of the CD45- fraction has been focused on the epithelial population this quarter.

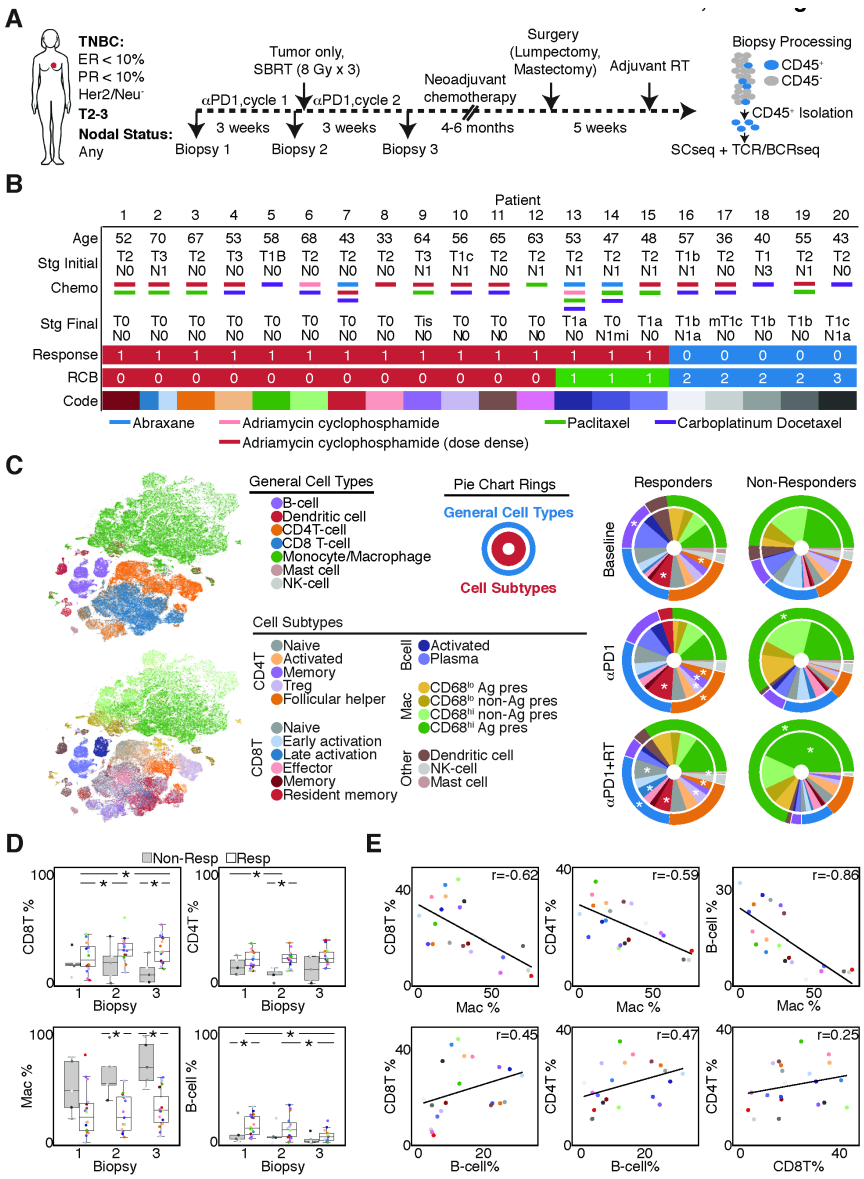

Figure 7. Single cell profiling of longitudinal biopsies identifies the immune cell populations that are most important for a response to combination immunotherapy in triple negative breast cancers. A) Schematic of clinical trial indicating the times at which biopsies were obtained (left) and the biopsy processing protocol where single immune cells were isolated, and their RNA sequenced along with corresponding T and B-cell receptors (right). **B)** Patient demographics, staging prior and post treatment, individualized chemotherapy regimens, response based on pathological complete response, RCB and patient color code for all subsequent figures. Note, Patient 2 had two tumors at the time of diagnosis, and both were profiled in this study. **C)** tSNE embedding of complete dataset colored by either broad or specific cell type annotations, as well as their average proportions in the different biopsies after separation based on their corresponding response (* indicates greater average proportion versus other response category; $p \leq 0.05$, rank-sum test). **D)** $CD8^+$ T-cell, $CD4^+$ T-cell, macrophage and B-cell proportions in the biopsies from responsive and non-responsive patients (* $p \leq 0.05$, rank-sum test between response and paired rank-sum test between biopsies). **E)** Spearman correlations between different T-cell types as observed in baseline biopsies.

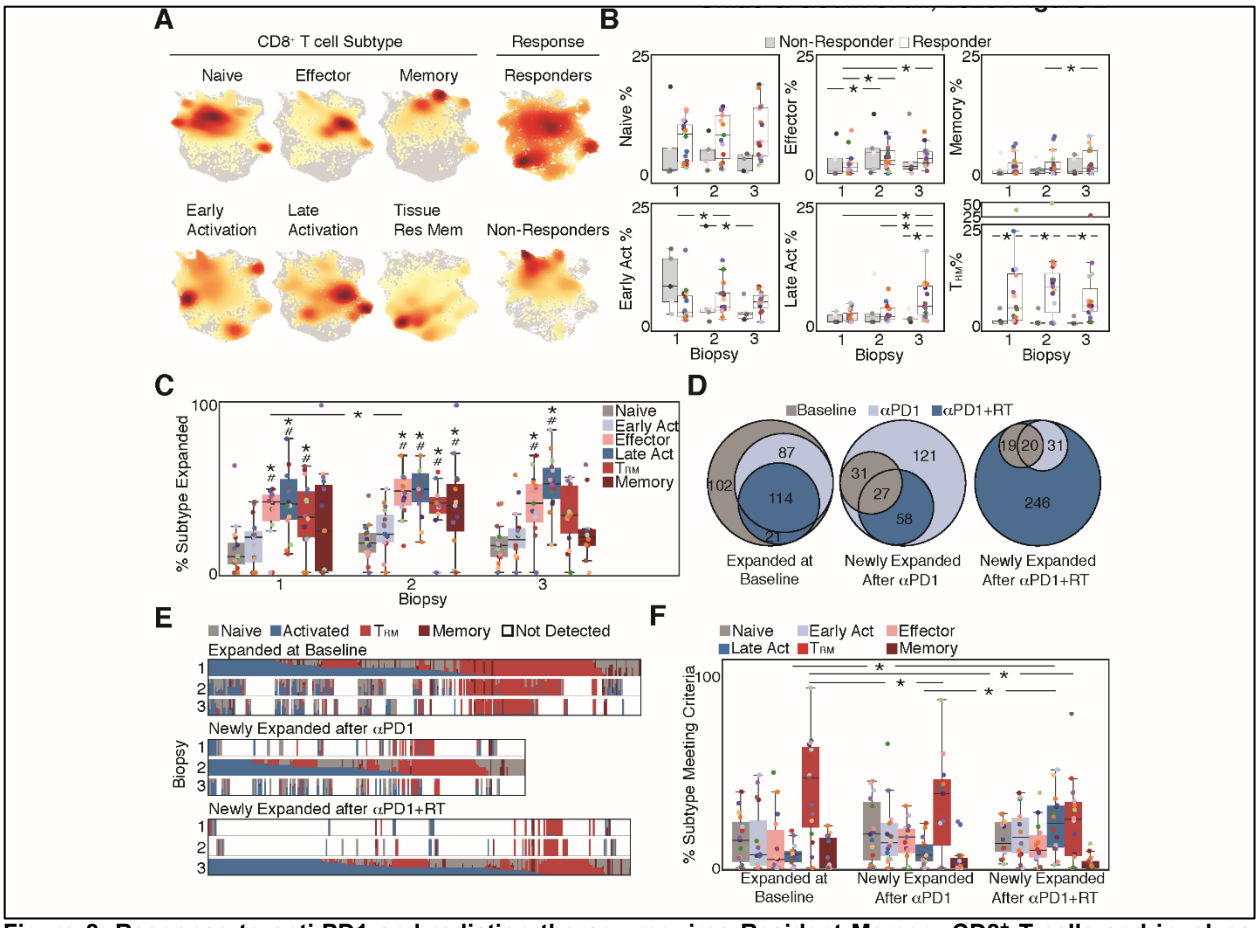

Figure 8. Response to anti-PD1 and radiation therapy requires Resident Memory CD8⁺ T-cells and involves an expansion of new activated CD8⁺ clonotypes. **A)** Density of cells within each subtype or within responders/non-responders overlaid on the UMAP embedding of all CD8⁺ T-cells. Responders and non-responders were subsampled to have equal numbers of cells before calculating the density. **B)** Proportions of each CD8⁺ T-cell subtype in each biopsy, where biopsies are separated based on corresponding response, * $p \leq 0.05$, rank-sum test between response and paired rank-sum test between biopsies. **C)** Percentage of cells from each CD8⁺ T-cell subtype that are expanded in each biopsy (* and # indicate rank-sum test $p \leq 0.05$ versus naïve and early activation, respectively, unless denoted by horizontal bars) **D)** Venn diagram representing the number of unique clonotypes expanded in each biopsy and whether they were identified in the other biopsies from the same patient. Clonotypes in the overlaps were detected in two or more biopsies. **E)** Tracking of clonotypes represented in **D** where each bar corresponds to a unique clonotype along with its phenotypic distribution and can be tracked down through the biopsies where it was detected. **F)** Subtype proportions of expanded clonotypes for each biopsy where expansion was not observed for that clonotype in the previous biopsy. For baseline, all expanded clones at baseline are included. * indicates $p \leq 0.05$ with paired rank-sum test.

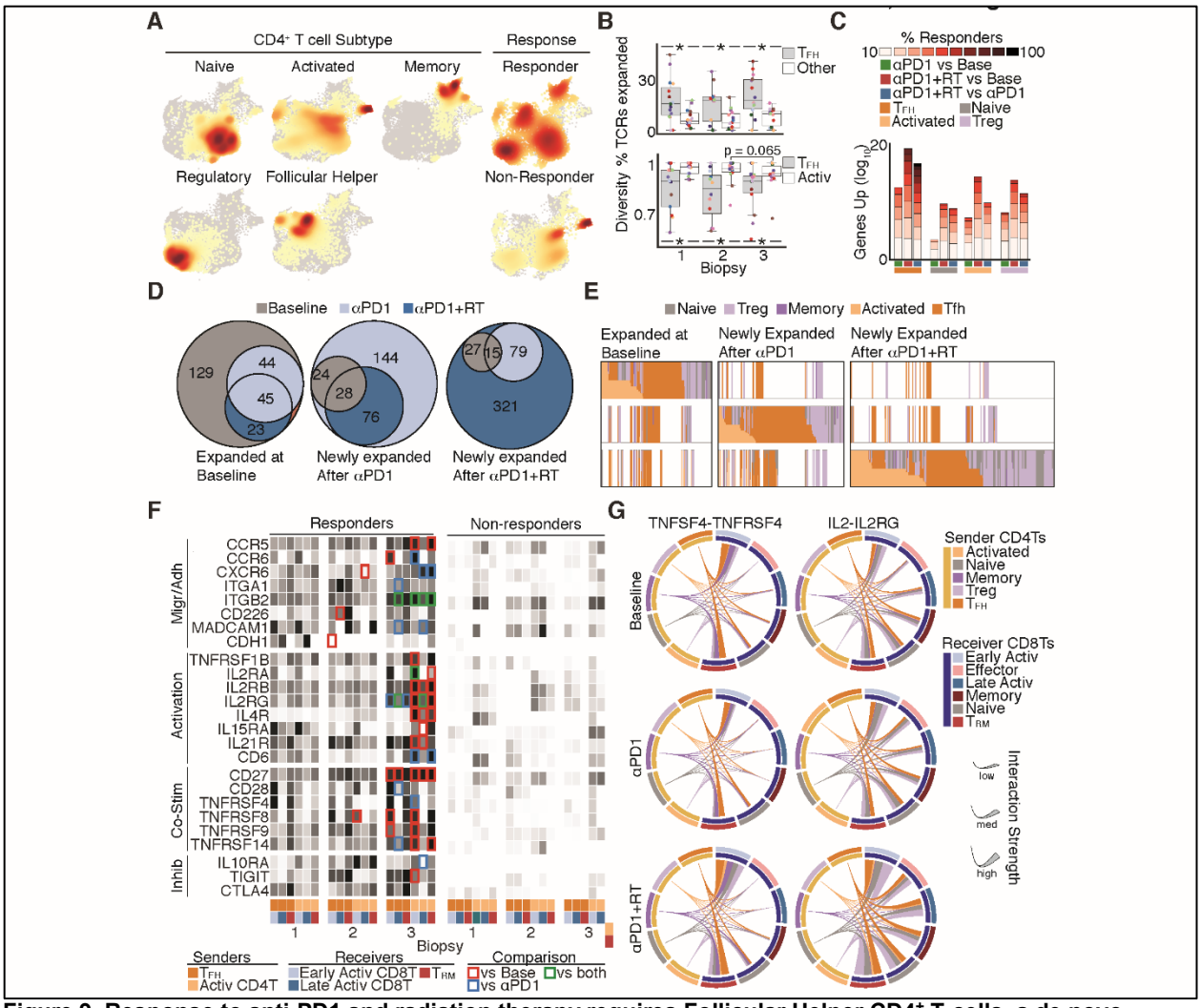

Figure 9. Response to anti-PD1 and radiation therapy requires Follicular Helper CD4⁺ T-cells, a de novo expansion of activated CD4⁺ T-cells and their interaction with activated and resident memory CD8⁺ T-cells. A) Density of cells within each subtype or within responders/non-responders overlaid on the UMAP embedding of all CD4⁺ T-cells. Responders and non-responders were subsampled to have equal numbers of cells before calculating the density. **B)** The percentage of clonotypes identified as expanded and the clonotype diversity of the indicated CD4⁺ subtypes, * indicates $p \leq 0.05$, rank-sum test. **C)** The cumulative number of genes upregulated by each treatment in each subtype, and the proportion of responders in which the change was observed. **D)** Venn diagram representing the number of unique clonotypes expanded in each biopsy and whether they were identified in the other biopsies from the same patient. Clonotypes in the overlaps were detected in two or more biopsies. **E)** Tracking of clonotypes represented in **D** where each bar corresponds to a unique clonotype along with its phenotypic distribution and can be tracked down through the biopsies where it was detected. **F)** Ligand-receptor interaction scores for different CD4⁺ T-cell (senders) and CD8⁺ T-cell (receivers) subtypes, where the interaction strength between the pair was altered by treatment and a functional implication is known. The colored edges indicate $p \leq 0.05$, rank-sum test. **G)** Circos plots depicting the strength of TNFSF4- and IL2-based interactions between all CD4⁺ T-cell (senders) and CD8⁺ T-cell (receivers) subtypes in biopsies from responding patients.

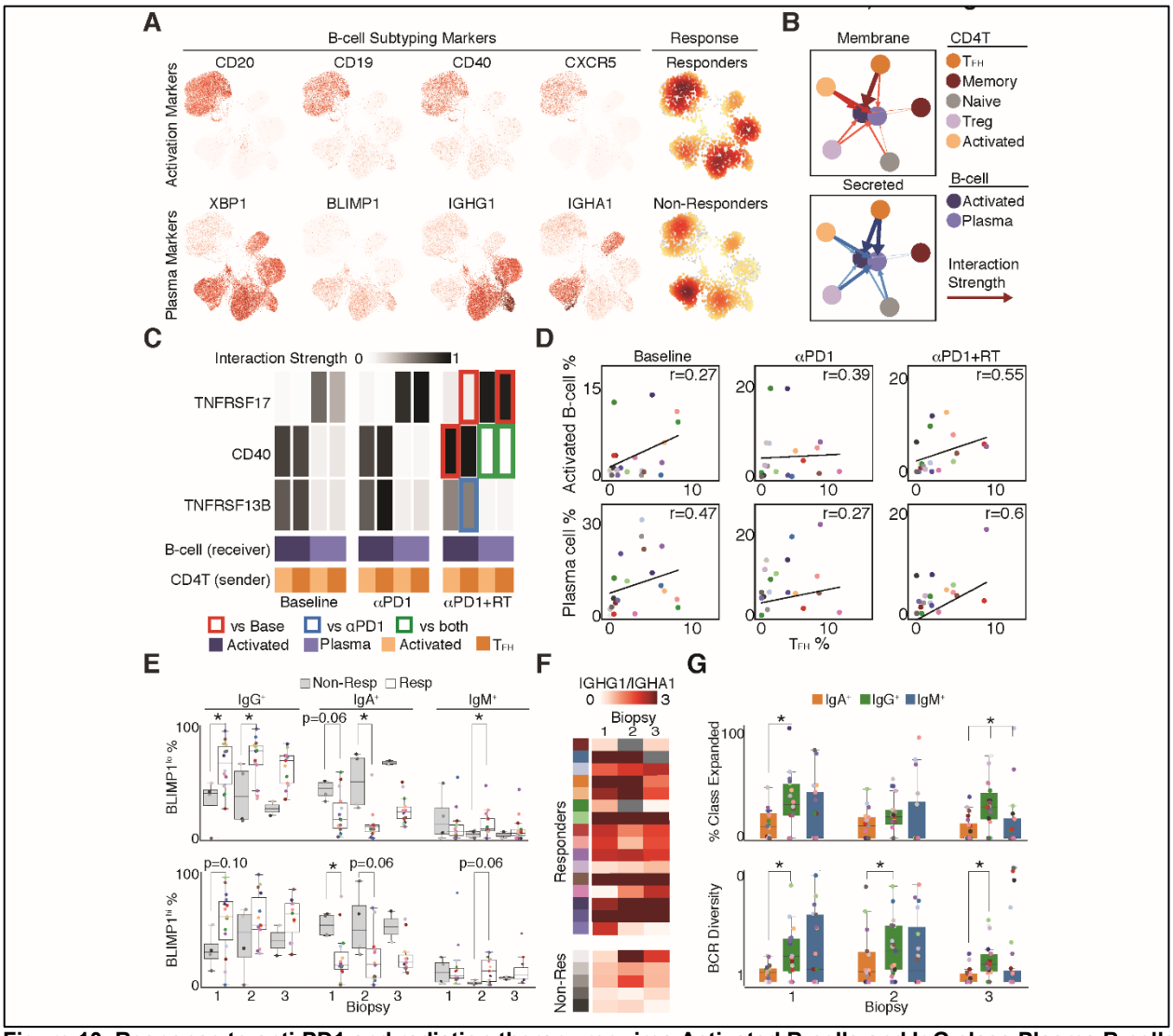

Figure 10. Response to anti-PD1 and radiation therapy requires Activated B-cells and IgG class Plasma B-cells that receive ligand signals from Follicular helper and Activated CD4⁺ T-cells. A) UMAP embedding of B-cells colored by expression of key phenotypic markers (left) or with density of cells from responders/non-responders overlaid (right). Responders and non-responders were subsampled to have equal numbers of cells before calculating the density. **B)** Ligand-receptor interaction strengths between each CD4⁺ T-cell subtype (sender) and each B-cell subtype (receiver) in responding patients. **C)** Heatmap showing the strengths of interactions between Activated or Follicular Helper CD4⁺ T-cells and Activated or Plasma B-cells that were altered by treatment in responders. The colored edges indicate $p \leq 0.05$, rank-sum test. **D)** B-cell subtype Spearman correlations with Follicular Helper CD4⁺ T-cells for each biopsy. **E)** Percentage of BLIMP1 expressing and non-expressing Plasma B-cells that fall into each Ig class for each biopsy in responding and non-responding patients, * $p \leq 0.05$, rank-sum test. **F)** Heatmap of the ratios of IGHG1/IGHA1 expression in the Plasma B-cells of responding and non-responding patients in each biopsy. **G)** Percentage of expanded cells and the diversity for each Plasma B-cell Ig class, in each biopsy, * $p \leq 0.05$, rank-sum test.

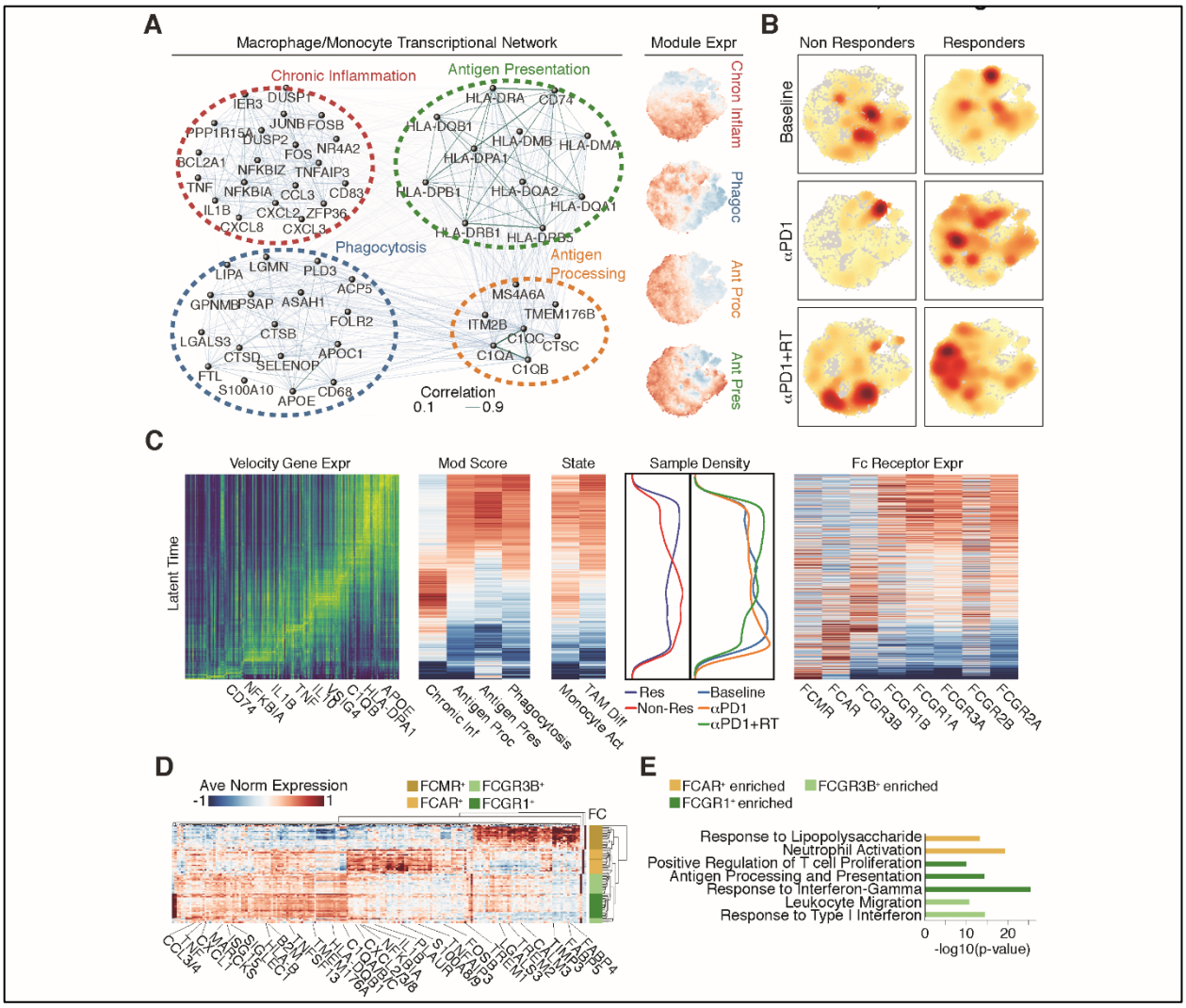

Figure 11. Response to anti-PD1 and radiation therapy requires macrophages transition to an antigen processing and presenting state that is linked to the expression of Fc receptors FCGR1A and FCGR1B. A) Gene regulatory network for macrophages as inferred through pairwise gene correlation analysis (left) and UMAP embedding of macrophages colored by network module score (right). **B)** Density of responders and non-responders in the UMAP embedding described in **A**. **C)** RNA velocity-based ordering of macrophages showing how latent time correlates with response, treatment, known phenotypic state, transcriptional module scores and Fc receptor expression. **D)** Clustering of macrophages based on genes identified as significantly (FDR ≤ 0.05) upregulated in any Fc receptor macrophage class as compared to all remaining macrophages. **E)** Gene Ontology terms enriched in the genes described in **E**.

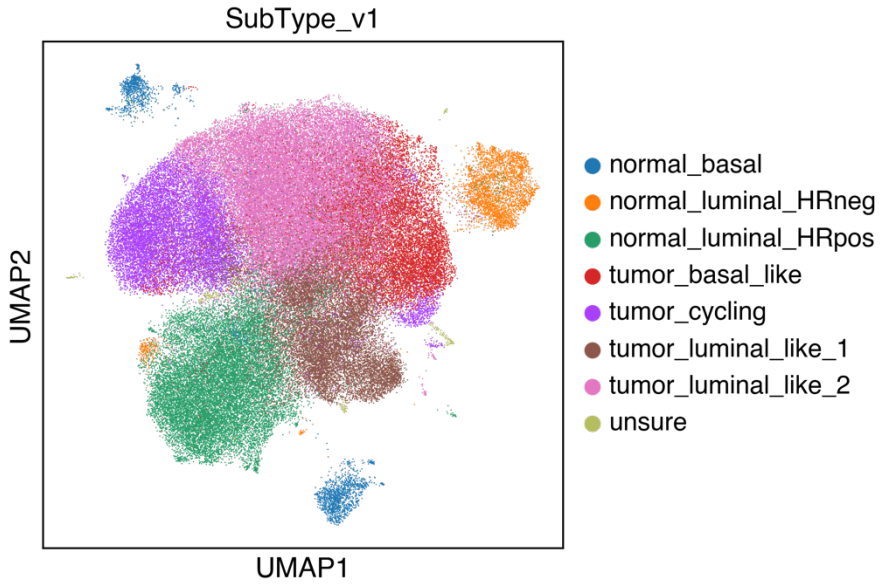

Figure 12. Annotated epithelial cell types. Based on known lineage marker expression we have annotated all cells in the epithelial compartment. We see normal basal, luminal HR- and luminal HR+ populations. Additionally, a large set of tumor cells with markers indicating cells their cell of origin to be one of the normal cell populations above, as well as a cycling population with high Ki67 expression.

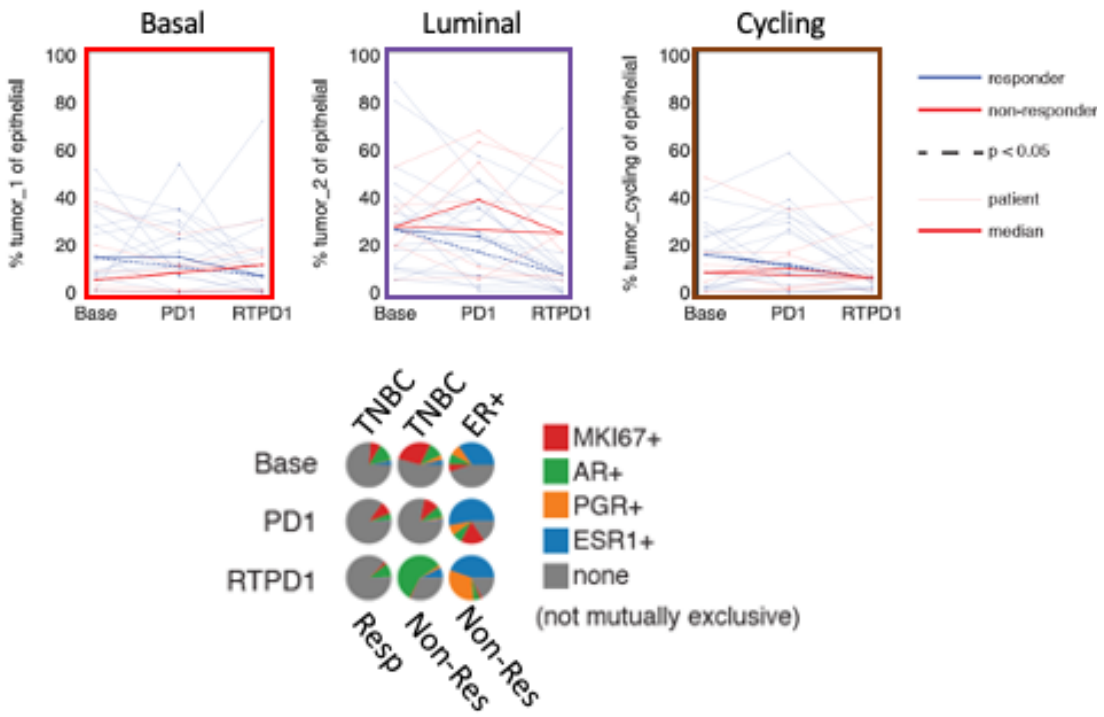

Figure 13) Epithelial cell representations across each patient biopsy showing alternative hormone regulation in luminal cells. We have studied each malignant epithelial cell population for their proportions across each of the three biopsies. We have found luminal HR- cells are most prominent in non-responding TNBC patients after the combination of radiation therapy and pembrolizumab. In studying the luminal tumor cell populations in the TNBC patients and in a separate cohort of ER+ patients we are analyzing for a separately funded project, we have found that non-responding tumors begin to express alternative hormone receptors after the combination therapy. Luminal HR- cells (lacking ER and PGR expression) from non-responsive tumors turn on the Androgen Receptor (AR) whereas Luminal HR+ cells (expressing ER) turn on the progesterone receptor.

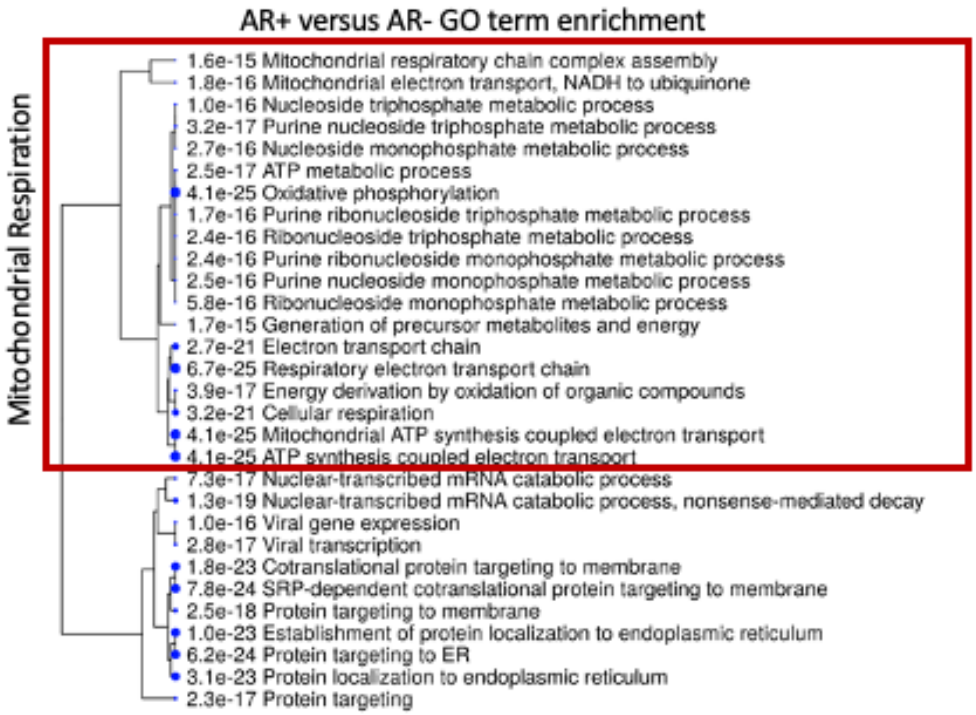

Figure 14) To study the molecular consequences of this hormone receptor activation, we performed a differential gene expression analysis between luminal tumor cells from TNBC tumors that expressed AR in the final biopsy, as compared to luminal tumor cells lacking AR expression from the same biopsies. This analysis identified numerous genes and corresponding pathways as being upregulated in response to AR activation. However, the strongest association was with mitochondrial respiration indicating these cells have altered their energy usage patterns in response to combined therapy. Numerous therapeutics exist that could target these response mechanisms, for example drugs that block AR signaling have and are being tested in multiple clinical trials and metabolic drugs exist that could help target mitochondrial respiration.

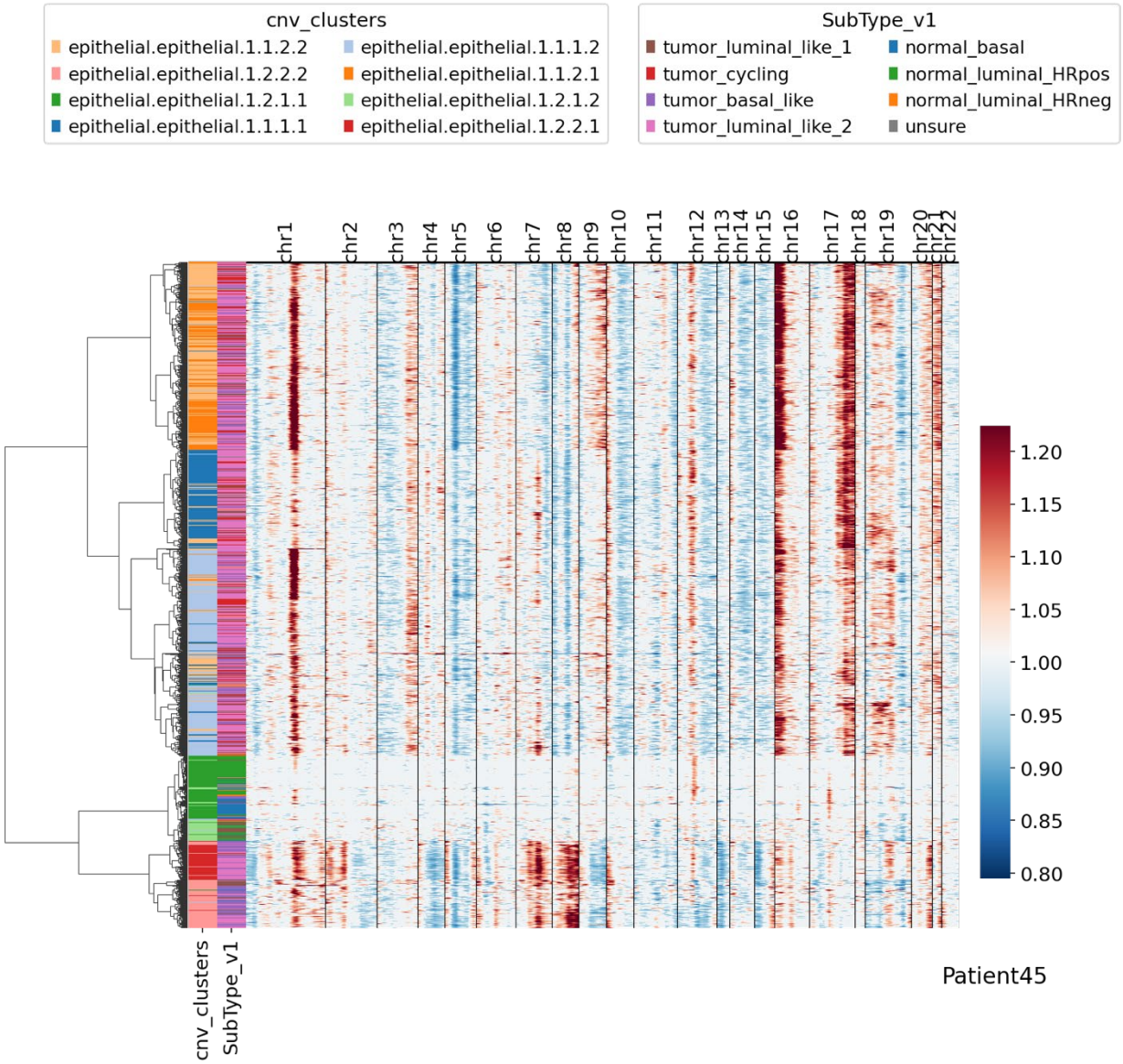

Figure 15) Inferred copy number changes in individual epithelial cells. We have inferred copy number changes for epithelial cells using the inferCNV software package, using fibroblasts and immune cells as a background set from which to call the copy number variations. Calls made on this specific patient indicate there are multiple clonal populations with the normal epithelial cells showing no copy number changes. One set of clones with a large portion of Chr7 and Chr8 are seen (epithelial.epithelial 1.2.2.2 & epithelial.epithelial 1.2.2.1), with the other clones seeming to have amplified arms of Chr16, Chr17 (epithelilial.epithelial 1.1.2.2, 1.1.1.1, 1.1.1.2 and 1.1.2.1). We are currently applying this method to track clonal cancer cell populations in each tumor throughout treatment to determine if specific clonal populations emerge after therapy.

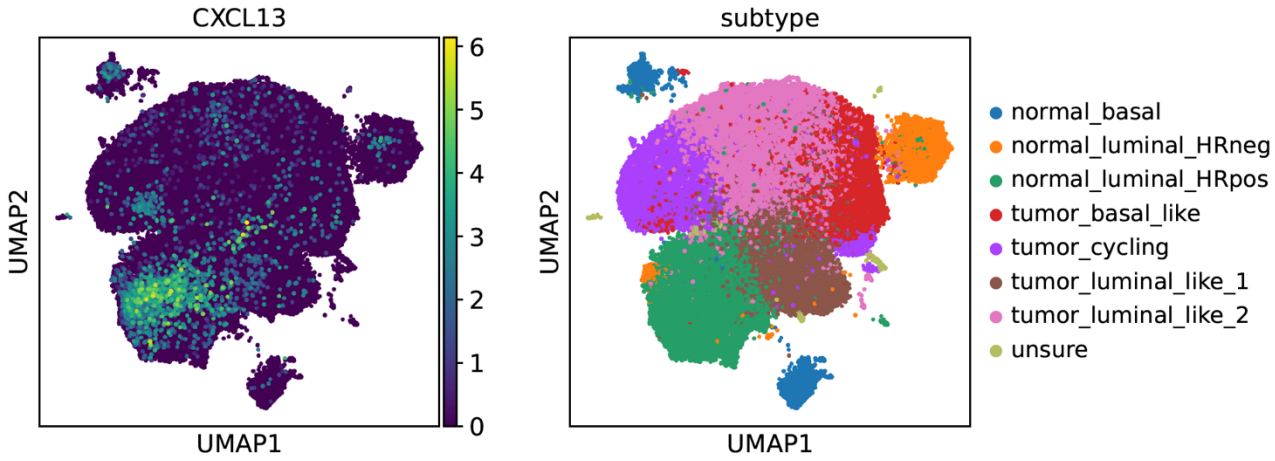

Figure 15) A normal CXCL13 luminal HR+ epithelial population.

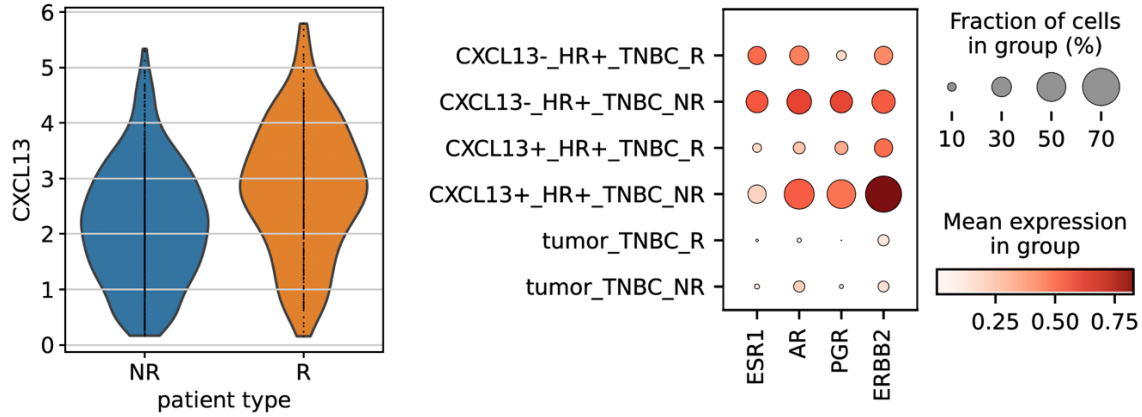

Figure 16) Left) CXCL13 expression in non-responder (blue) and responder CXCL13 expressing normal luminal HR+ epithelial cells (p-value <0.005). **Right)** Hormone receptor expression profile of different tumoral epithelial populations in TNBC tumors.

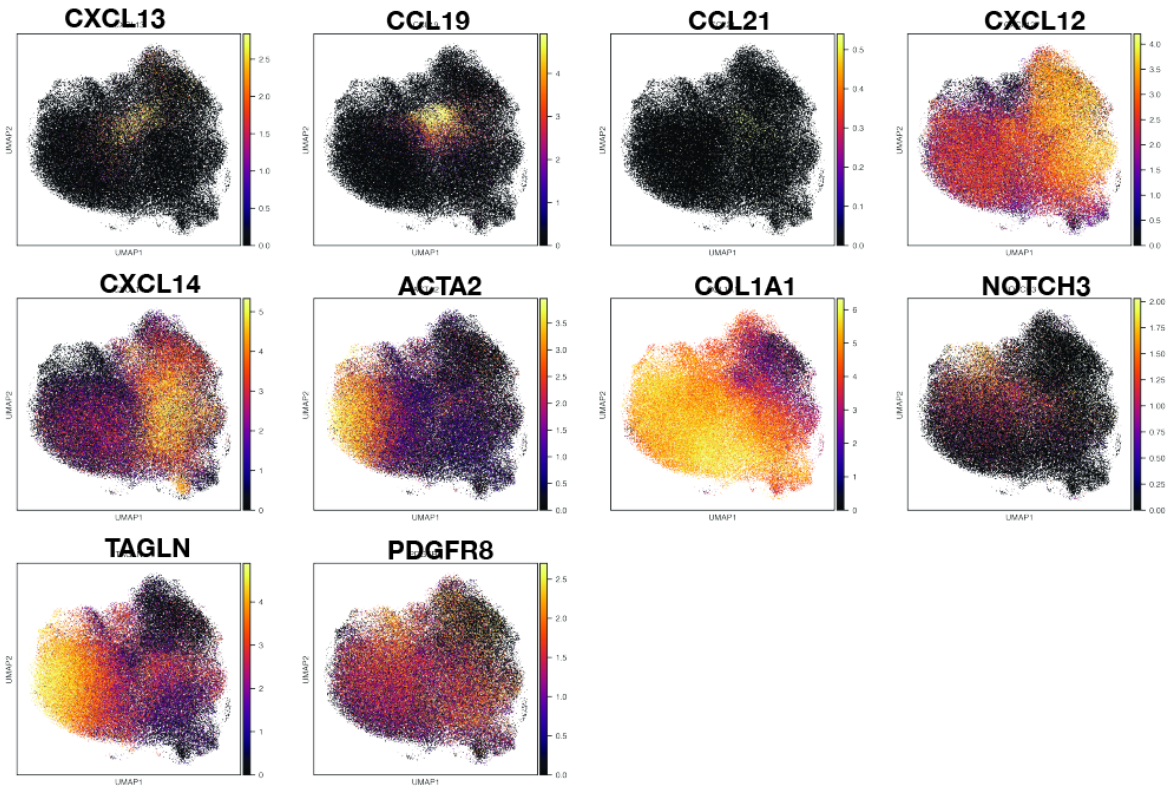

Figure 16) Marker expression in the fibroblasts identified in the TNBC tumors.

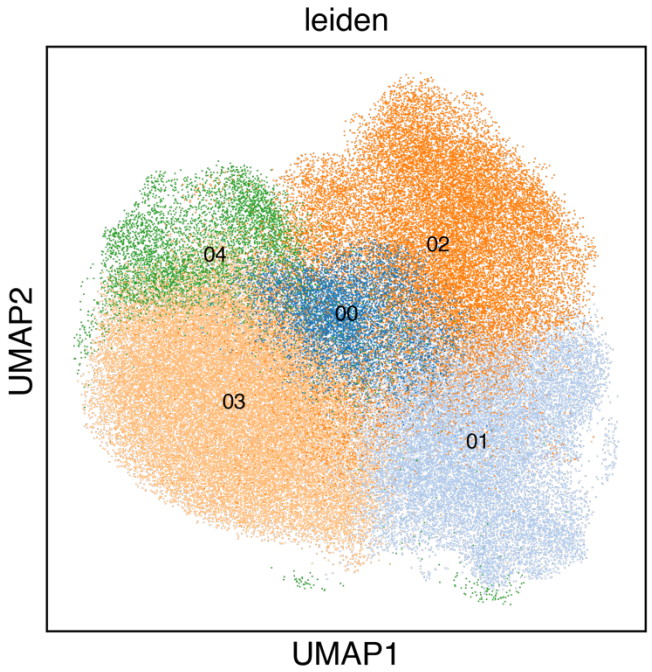

Figure 17) Unbiased clusters called in the fibroblast populations.

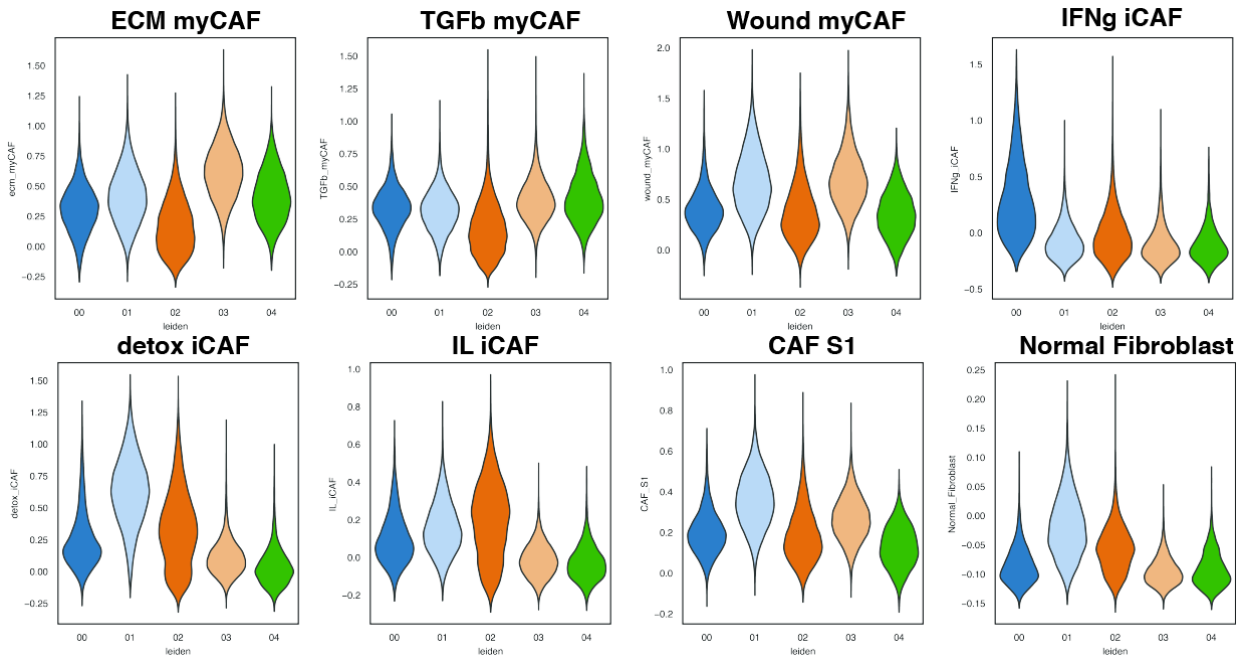

Figure 11) Annotation of the fibroblast clusters based on their signature scores according to Grigariou et al, 2019. We are currently studying these fibroblast groups for their proportion differences and in responding and non-responding patients and how they change over time with therapy.

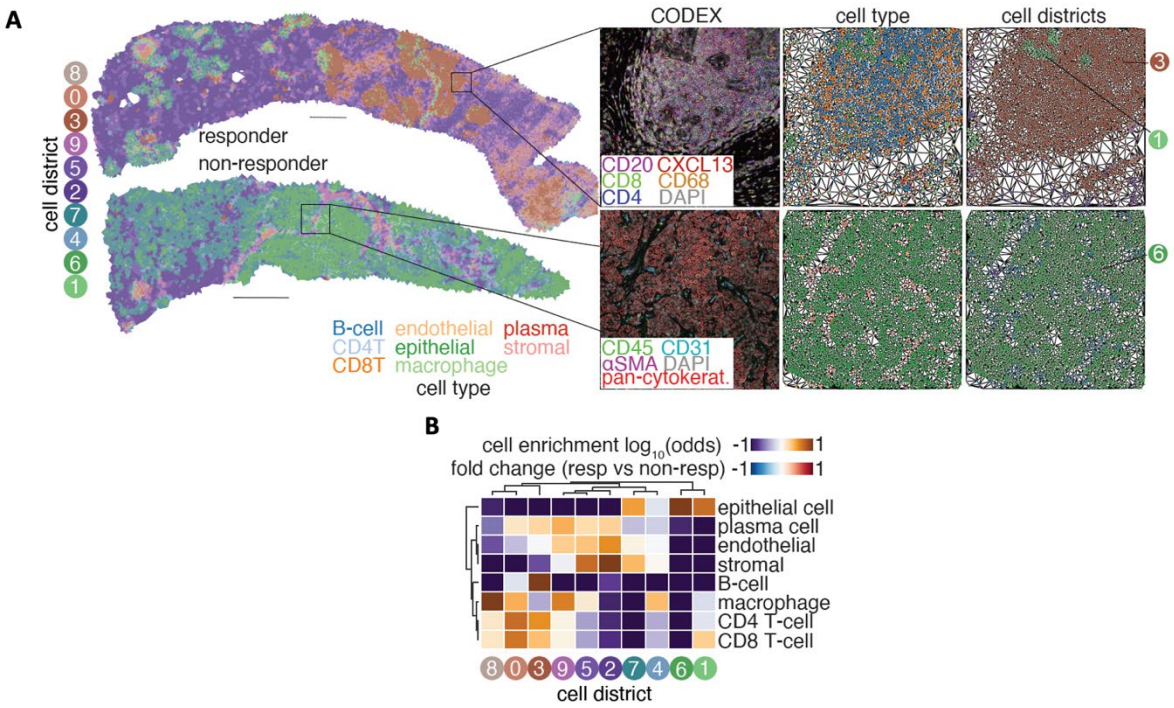

Figure 18. Multiplex immunohistochemistry analysis for immune cells using CO-Detection by indEXing (CODEX) Biopsies obtained from the pembrolizumab and radiation clinical trial in TNBC were analyzed using CODEX and major cell classes (immune and non-immune) were identified using their canonical markers (A). Relationship between the immune cells were determined by measuring the distance between different cell types and nine “neighborhoods” were identified by clustering that consisted of different mixtures of the 8 major cell types (B).

We started our analysis of the immune compartments examining T and B cells (Figure 8, 9, 10), T cell receptor (TCR) and B cell receptor (BCR) sequencing allowed us to analyze clone dynamics in the context of global gene expression signatures. BCRs followed expected kappa/lambda usage distributions, with combination treatment inducing more unique lambda chain BCRs, and expanded B-cells differentially expressed specific immunoglobulin Fc units (IgG versus IgA), suggesting increased antibody production of specfici subtypes in responding versus non-responding patients (Figure 10).

Naïve CD8Ts were moderately increased in proportion following pembrolizumab, and memory cells were slightly enriched after the combination therapy (Figure 8). However, an advanced activation CD8 T-cell phenotype increased following combination treatment. This phenotype comprised both activation (Perforin, GZMB) and exhaustion (LAG3, TIM3) genes along with previously described tumor-reactive markers such as CD103 and CXCL13. Transition probabilities calculated on TCRs present in the last two biopsies revealed RT could stimulate pre-existing clonotypes to display this signature regardless of their prior subtype distribution. However, many newly expanded TCRs were also detected after RT, driving an increase in the overall proportion of expanded cells in the CD8T population (Figure 8C). Most importantly, these newly established clonotypes, like the expanded set in general, were found to be enriched for cells of the advanced activation subtype (Figure 8F).

Within the CD4T population we found seven cell phenotypes, which were unchanged in proportion by either the single or combination treatment (Figure 9). However, RT induced expression of many regulatory genes in human Tregs where corresponding orthologs were also upregulated in murine iTregs. Expanded CD4Ts were reduced in naïve and early activated phenotypes and increased in Th2 regulatory cell proportion. However, treatment did not induce expansion of CD4Ts.

To analyze human macrophages, we averaged pairwise gene correlations from each patient tumor and applied thresholding to develop a co-expression network (Figure 11). This identified a three-module network bearing strong resemblance to the murine transcriptional system. One module overlapped with the murine suppressive subnetwork, but for a lack of interferon response genes. Furthermore, MHC class II genes, including murine orthologs CD74 and HLA-DQB1, were harbored in a second component. The remaining subnetwork overlapped strongly with the murine phagocytic module, with both harboring the same tightly correlated complement pathway gene set. The lack of the recruitment subnetwork may reflect the later timepoint of the biopsy compared to the preclinical model, since this subnetwork was most evident at Day 3 following RT. When macrophages were categorized based on network gene expression levels, three classes emerged where cells from each group had maximal activity for a specific transcriptional module. Phagocytic and suppressive cells were represented in all patients, but only seven tumors harbored the antigen presenting population. When temporal trajectories were calculated for these cells, it was inferred that human macrophages infrequently transitioned between phagocytic and suppressive states, indicating the population changes observed were likely due to newly recruited monocytes differentiating into a specific phenotype (Figure 11C).

We followed intratumoral macrophage proportions and found pembrolizumab induced moderate changes, including increased phagocytic and decreased suppressive cell proportions (Figure 11B). Combination therapy significantly amplified this shift to a phagocytic phenotype compared to anti-PD-1 alone. Additionally, the antigen presenting population was increased following administration of the combination therapy. When comparing global gene expression differences, we found the baseline population exhibited a suppressive phenotype, whereas pembrolizumab treated tumors harbored more of the phagocytic macrophage phenotypes. In contrast, macrophages from RT and pembrolizumab treated tumors maximally express the complement and antigen presentation transcriptional modules. Interestingly, macrophage phenotype was also associated with their antibody receptors with FCGR1A associated with antigen

presenting phenotype and FCAR associated with immunosuppressive activity (Figure 11C, D, E). We also initiated spatial analysis of the biopsies to help identify the 3D-localization of the various immune and non-immune cells (Figure 12). We began this analysis by identifying 9 different cell "districts" characterized by associations between different immune and non-immune cells. As expected many of the responding patients had immune-rich districts while non-responders were dominated by non-immune districts.

In this year, we also began analysis of the non-immune (CD45-) compartment using single-cell sequencing and found that we were able to identify distinct clusters among the tumor cells associated with hormone-receptor, luminal cell markers and tumor cell cycling (Figure 13). When we analyzed these cells across time found the luminal populations were most abundant following RT in non-responders (Figure 14). Further, an analysis of this population showed that in non-responders luminal cells activate the androgen receptor (AR, Figure 14), with a result of having an increased level of mitochondrial respiration, which we now believe is a key resistance mechanism for these tumors (Figure 15). Beyond studying cell proportion and gene expression changes, we are also now studying the clonal dynamics of the tumor cells in these lesions using methods to infer copy number changes, and then clustering cells by their inferred copy number profile (Figure 16).

Another major effort that we have begun is focused on the normal cells within TNBC tumors, beyond just immune cells. Given the enrichment of TFH and TRM in responding tumors, and the fact that both of these populations express the ligand CXCL13 to likely recruit B cells to for tertiary lymphoid structures in the tumor, we were very interested when we found a number of CXCL13 expressing epithelial cells within the normal luminal HR+ epithelial group (Figure 17). More interesting, in responder these cells express CXCL13 at higher levels than in non-responders, and in addition in non-responders these cells express an alternative hormone receptor expression profile, characterized by ERRB2 expression, whereas in responders very little hormone receptor expression is seen in this population at all (Figure 17). Our current hypothesis is these cells are responding to tissue damage inside of the tumor and act as a sensor to this damage, with the goal of recruiting B cells through CXCL13 to form tertiary lymphoid structures. Beyond this we have also been studying the CAF populations in these tumors and have identified a CXCL13 positive population in there, which we believe are reticular fibroblasts that are the structural foundation of lymph nodes and what we believe are helping to form TLSs in the tumor.

Summary of Results

Our studies demonstrate that RT can alter the immune microenvironment of breast tumors in a characteristic pattern and that adding RT to anti-PD-1 therapy leads to a more productive cytotoxic anti-tumor immune response, consistent with human and murine studies[13,16,17]. Most importantly, we found that following RT combined with pembrolizumab, irrespective of the starting immune composition, nearly 80% of the patients examined demonstrated new and activated CD8 T cell clones compared to less than 20% with pembrolizumab alone, which mirrors previous clinical data for pembrolizumab. These results suggest that RT sensitizes breast tumors to checkpoint blockade by producing new T cell clones and encouraging their activation through the stimulation of key anti-tumor pathways including type I interferons, which have been previously identified as essential mediators of RT-induced inflammation.

Our most intriguing finding was the discovery of a specific macrophage phenotype that occurs following RT. Previous studies have suggested that eliminating macrophages enhances the response to RT in breast, glioblastoma and head and neck cancers. This current study suggests these successes resulted from targeting the immunosuppressive activity of macrophages triggered in the later phases following RT. However, our study revealed macrophages that enter tumors immediately following RT are largely inflammatory and primed to kill damaged cells through their expression of complement. Over the course of a week though, these cells gradually acquire increasing immunosuppressive capacity as they restore tumor hemostasis. During this process

macrophages strongly upregulate their digestive pathways and express multiple proteins suggesting elevated phagocytosis and antigen presentation. We hypothesize the synergy between RT and anti-PD-1 therapy lies in the ability to retain killing and antigen presenting capacity while preventing suppressive activity. This hyper-phagocytic phenotype likely transitions to an immunosuppressive one eventually, as macrophages eating apoptotic bodies exhibit increased immunosuppressive capacity. Our findings, further highlight the idea that phagocytic checkpoints are critical in regulating tumor responses in part through their ability to regulate macrophage suppressive capacity and are associated with specific antibody production.

Thus, in this study we characterize the entire immune landscape of breast tumors following RT and show that there are dramatic changes in the numbers, but more importantly, the functional phenotype and now spatial distribution of the intratumor immune cells. In both preclinical models and patients, we find that targeting the suppressive activity induced by RT using anti-PD-1 therapy leads to significant synergistic increases in cytotoxic activity beyond RT or anti-PD-1 alone. These findings suggest that RT combined with PD-1/PD-L1 directed therapy converts unresponsive breast tumors to responsive ones in the neoadjuvant setting.

What opportunities for training and professional development has the project provided?

Nothing to report

How were the results disseminated to communities of interest?

In addition to the project meetings relevant members of the Knott and Shiao labs attend, we also hold general joint laboratory meetings where we discuss the multiple shared projects between our two labs. We have invited and our consumer advocate Michele Rakoff has joined these monthly meetings up until they were canceled due to Covid-19. As we begin these meetings again Michele will be invited to join and to begin to disseminate our results to the advocate and patient community.

What do you plan to do during the next reporting period to accomplish the goals?

Our mouse projects have now resumed so a major focus going forward will be pushing to complete the single-dose as well as the multi-dose in two tumor experiments to study abscopal responses. We will also begin to look into the mechanism of these responses by depleting the various different cell types. Further, we will also continue our analysis of the non-immune (CD45-) fractions of these tumors to understand how the tumor cells, fibroblasts and endothelial cells are changed by the combined therapy and how these cells may be influencing other populations. We also hope to incorporate spatial information about all of these cells into our analysis to better understand the post-treatment tumor dynamics.

In terms of clinical studies, we will continue to accrue patients into our phase II trial. We expect that the number of patients will begin to reach levels where more definitive comparisons can be made between responders and non-responders in terms of their immune composition. Further, like with the murine data we will begin to delve deeper into the B-cells and other immune populations in these tumors, and we will begin to analyze the CD45- fractions of these tumors. We will continue to incorporate more information about the ligand and receptor interactions between different immune and stromal populations so that the cellular interactions governing response can be uncovered.

4. IMPACT:

What was the impact on the development of the principal discipline(s) of the project?

Our single cell analysis of the murine and human tumor microenvironment and in particular the macrophage population has allowed us to better describe the transcriptional machinery shaping the phenotypic heterogeneity of each immune cell population. This is particularly true for macrophages, whose categorization into pro-tumor M1 or anti-tumor M2 groups previously has been controversial and generally regarded as not capturing their full phenotypic plasticity. Our analysis of murine and human macrophages has identified four module transcriptional regulatory networks that regulate these populations with similar modules being contained in each network, such as ones regulating inflammation and suppression, phagocytosis, and antigen presentation. We found that radiation strongly induces expression of the phagocytosis and antigen presentation modules and that the addition of anti-PD1 therapy increases expression of these modules. We hypothesize that antigen presentation by these cells after RT is a reason for why there is an increased number of novel CD4+ and CD8+ T cell clones in the tumor.

In terms of clinical practice, our mouse studies and our early clinical studies indicate that the combination of anti-PD1 therapy and RT in the neoadjuvant setting for women with TNBC results in significantly increased rates of pathological complete or near complete response compared to historical value for chemotherapy alone (Cortazar *Lancet* 2014). If this trend continues in the remaining patients it would indicate the combination is a valid alternative to the combination of anti-PD1 therapy and chemotherapy that was recently reported to increase response rates to 64% (KEYNOTE-522, Schmid NEJM 2020). The phase Ib portion also revealed that the proposed strategy is also safe with no additional reported surgical complications (wound healing, infection) and one Grade 3 skin reaction and one Grade 4 incidence of colitis. Thus, from initial portion of this trial, we determined that our strategy as it stands is safe and may have potential efficacy so we determined with the Institutional Review Board and Data Safety Monitoring Committee to proceed with the phase II portion of the trial which is currently underway despite minor delays from COVID restrictions.

What was the impact on other disciplines?

Our description of tumoral macrophages and how they regulate immunotherapy response is likely also valid for other tumors such as lung tumors where novel new CD8+ T cell clones are also observed after anti-PD1 therapy with RT, like we see here. More broadly, the transcriptional modules that we have identified as being important for the plastic nature of macrophages are also likely valid for macrophages in other tumors, and perhaps diseases, and these modules could be an area of further studies in those tumors and diseases.

This is a novel strategy incorporating RT upfront in the neoadjuvant setting for triple-negative breast cancer. Thus far, we have determined that it was safe and now we are studying whether it is efficacious compared to the standard of care. This paradigm will change the way RT is incorporated into breast cancer and also have implications for multiple cancers and how they incorporate RT and immunotherapy.

What was the impact on technology transfer?

Nothing to report

What was the impact on society beyond science and technology?

Nothing to report

5. CHANGES/PROBLEMS:

Changes in approach and reasons for change
Nothing to Report

Actual or anticipated problems or delays and actions or plans to resolve them

We continued to experience a several month delay in our murine experiments and a slowed clinical accrual as a result of COVID19 in the first half of this year. Due to the laboratory and clinical trial operation shut down we did not complete everything we had hoped to over the past year, but have planned ahead by requesting and, fortunately, receiving cost extension to complete our work. Things have since resumed near normal operations and thus we do not anticipate any further delays.

Changes that had a significant impact on expenditures
Nothing to Report

Significant changes in use or care of human subjects, vertebrate animals, biohazards, and/or select agents

Significant changes in use or care of human subjects
Nothing to Report

Significant changes in use or care of vertebrate animals
Nothing to Report

Significant changes in use of biohazards and/or select agents
Nothing to Report

6. PRODUCTS:

- **Publications, conference papers, and presentations**

  Journal publications.

  Books or other non-periodical, one-time publications.

  Other publications, conference papers and presentations.

Poster Presentation at San Antonio Breast Cancer Conference (2019):
H. McArthur *et al.*, Abstract P2-09-07: Preoperative pembrolizumab (Pembro) with radiation therapy (RT) in patients with operable triple-negative breast cancer (TNBC). *Cancer Research* **79**, P2-09-07-P02-09-07 (2019).

- **Website(s) or other Internet site(s)**
  Nothing to Report

- **Technologies or techniques**
  Nothing to Report

- **Inventions, patent applications, and/or licenses**
  Nothing to Report

- **Other Products**
  Nothing to Report

7. PARTICIPANTS & OTHER COLLABORATING ORGANIZATIONS

What individuals have worked on the project?

Name:	Simon Knott
Project Role:	Partnering Principal Investigator
Researcher Identifier (e.g. ORCID ID):	
Nearest person month worked:	2.64
Contribution to Project:	Dr. Knott supervised the development and analysis of single cell libraries from mouse tumor models and human tumor biopsies.
Funding Support:	Institutional Support

Name:	Aagam Shah
Project Role:	Research Associate I
Researcher Identifier (e.g. ORCID ID):	N/A
Nearest person month worked:	3.12
Contribution to Project:	Aagam Shah has developed and is developing computational pipelines for processing single cell data from mouse tumor models and human tumor biopsies.
Funding Support:	Institutional Support

Name:	Andrew Martinez
Project Role:	Research Associate I

Researcher Identifier (e.g. ORCID ID):	N/A
Nearest person month worked:	5.52
Contribution to Project:	Andrew Martrinez is helping to process the samples from the clinical trial for sequencing and immunohistochemistry validation experiments.
Funding Support:	Institutional Support

Name:	Nathan Ing
Project Role:	Research Bioinformatician
Researcher Identifier (e.g. ORCID ID):	N/A
Nearest person month worked:	4.68
Contribution to Project:	Nathan has developed and is developing computational pipelines for processing single cell data from mouse tumor models and human tumor biopsies.
Funding Support:	Institutional Support

Name:	Bassem Ben Cheikh
Project Role:	Research Bioinformatician
Researcher Identifier (e.g. ORCID ID):	N/A
Nearest person month worked:	2.52
Contribution to Project:	Bassem has developed and is developing computational pipelines for processing single cell data from mouse tumor models and human tumor biopsies.
Funding Support:	Institutional Support

Name:	Brianna Mulligan
Project Role:	Research Bioinformatician
Researcher Identifier (e.g. ORCID ID):	N/A
Nearest person month worked:	3
Contribution to Project:	Brianna has developed and is developing computational pipelines for processing single cell data from mouse tumor models and human tumor biopsies.
Funding Support:	Institutional Support

Name:	Catherine Oh
Project Role:	Research Bioinformatician
Researcher Identifier (e.g. ORCID ID):	N/A
Nearest person month worked:	2.4
Contribution to Project:	Catherine is helping to process the samples from the clinical trial for sequencing and immunohistochemistry validation experiments.
Funding Support:	Institutional Support

Name:	Ravleen Dehiya
Project Role:	Research Bioinformatician
Researcher Identifier (e.g. ORCID ID):	N/A
Nearest person month worked:	1.92
Contribution to Project:	Ravleen has developed and is developing computational pipelines for processing single cell data from mouse tumor models and human tumor biopsies.

Funding Support:	Institutional Support

Name:	Fleury Nsole-Biteghe
Project Role:	Postdoctoral Scientist
Researcher Identifier (e.g. ORCID ID):	
Nearest person month worked:	3.0
Contribution to Project:	Dr. Nsole-Biteghe helped write the IACUC protocol and work on the experimental protocols needed for the murine experiments.
Funding Support:	Department of Defense

Name:	Stephen Shiao
Project Role:	Partnering Principal Investigator
Researcher Identifier (e.g. ORCID ID):	0000-0001-7586-2885
Nearest person month worked:	0.6
Contribution to Project:	Dr. Shiao wrote the IACUC and clinical trial protocols and supervised the training of the personnel who will be conducting the mouse experiments, working on the clinical trial and processing the samples resulting from the clinical trial.
Funding Support:	Department of Defense, National Cancer Institute

Name:	Jolene Viramontes
Project Role:	Research Assistant I
Researcher Identifier (e.g. ORCID ID):	
Nearest person month worked:	1.5

Contribution to Project:	Jolene helps with processing of clinical specimens and has helped with beginning the process of analyzing the murine specimens.
Funding Support:	Department of Defense

Name:	Natalie-Ya Mevises
Project Role:	Research Assistant II
Researcher Identifier (e.g. ORCID ID):	
Nearest person month worked:	1.5
Contribution to Project:	Natalie-Ya Mevises has been assisting with development and refinement of the clinical and lab specimen processing.
Funding Support:	Department of Defense

Name:	Heather McArthur
Project Role:	Partnering Principal Investigator
Researcher Identifier (e.g. ORCID ID):	
Nearest person month worked:	0.125
Contribution to Project:	Dr. McArthur has been working on the development of the clinical trial protocol.
Funding Support:	Department of Defense

Name:	Scott Karlan
Project Role:	Partnering Principal Investigator
Researcher Identifier (e.g. ORCID ID):	

Nearest person month worked:	0.125
Contribution to Project:	Dr. Karlan has been assisting with the development of the clinical trial protocol, particularly the specifics of the specimen collection.
Funding Support:	Department of Defense

Has there been a change in the active other support of the PD/PI(s) or senior/key personnel since the last reporting period?
Nothing to Report

What other organizations were involved as partners?
Nothing to Report

8. SPECIAL REPORTING REQUIREMENTS

COLLABORATIVE AWARDS:

QUAD CHARTS:

9. APPENDICES: